HHS Public Access

Author manuscript

Mech Dev. Author manuscript; available in PMC 2021 December 01.

Published in final edited form as:

Mech Dev. 2020 December ; 164: 103644. doi:10.1016/j.mod.2020.103644.

The Cdx Transcription Factors and Retinoic Acid Play Parallel Roles in Antero-Posterior Position of the Pectoral Fin Field During Gastrulation

Christopher A. Quintanilla[a], **Robert K. Ho**[b]

[a]Committee on Developmental, Regeneration and Stem Cell Biology, University of Chicago, Chicago IL 60637 USA

[b]Department of Organismal Biology and Anatomy, University of Chicago, 1027E. 57th St, Chicago, IL 60637, USA

Abstract

The molecular regulators that determine the precise position of the vertebrate limb along the anterio-posterior axis have not been identified. One model suggests that a combination of *hox* genes in the lateral plate mesoderm (LPM) promotes formation of the limb field, however redundancy among duplicated paralogs has made this model difficult to confirm. In this study, we identify an optimal window during mid-gastrulation stages when transient mis-regulation of retinoic acid signaling or the *caudal* related transcription factor, Cdx4, both known regulators of *hox* genes, can alter the position of the pectoral fin field. We show that increased levels of either RA or Cdx4 during mid-gastrulation is sufficient to rostrally shift the position of the pectoral fin field at the expense of surrounding gene expression in the anterior lateral plate mesoderm (aLPM). Alternatively, embryos deficient for both Cdx4 and Cdx1a (Cdx-deficient) form pectoral fins that are shifted towards the posterior and reveal an additional effect on size of the pectoral fin buds. Prior to formation of the pectoral fin buds, the fin field in Cdx-deficient embryos is visibly expanded into the posterior LPM (pLPM) region at the expense of surrounding gene expression. The effects on gene expression immediately post-gastrulation and during somitogenesis support a model where RA and Cdx4 act in parallel to regulate the position of the pectoral fin. Our transient method is a potentially useful model for studying the mechanisms of limb positioning along the AP axis.

CRediT author statement

Christopher A Quintanilla: conceptualization, methodology, validation, formal analysis, visualization, investigation, project administration, writing-original draft, writing-review & editing preparation. **Robert K Ho**: conceptualization, methodology, resources, writing-original draft preparation, writing-review & editing supervision, project administration, funding acquisition

Declaration of competing interest

The authors declare that they have no competing interests.

1. Introduction

There appear to be constraints in place for the ultimate position of forelimbs in tetrapods as forelimb position corresponds to the vertebral region where cervical segments transition to thoracic segments. Earlier in development, when the developing forelimb is first visible as a limb bud, the limb bud position also appears to correlate with expression of *Hoxc6* in the somites (Burke et al., 1995). In contrast, the expression of *hoxc6* in the zebrafish embryo does not exactly correspond with where the pectoral fin bud forms and other possible factors that regulate the position of the pectoral fins are unknown. In addition, the time at which these factors act to determine pectoral fin position is unknown.

Retinoic Acid (RA) signaling plays a role in induction and patterning of numerous organs during vertebrate development (reviewed by Cunningham and Duester, 2015; Duester, 2008). In the Lateral Plate Mesoderm (LPM) of zebrafish, progenitors that give rise to blood vessels of the head are restricted by high levels of RA (Rydeen and Waxman, 2014). RA also plays a role in restricting the number of cardiac progenitors, and complete loss of RA results in an expansion of cardiac associated genes into more posterior LPM (pLPM) (Keegan et al., 2005). Embryos deficient in Aldh1a2, the enzyme that synthesizes most of the embryonic RA, fail to form pectoral fins (Begemann et al., 2001; Grandel et al., 2002). In contrast, embryos deficient in Cyp26a, the primary RA degradation enzyme in the early embryo, have a prolonged increase in RA and later form defects in pectoral fin patterning, outgrowth and potentially in antero-posterior (AP) position (Emoto et al., 2005).

The time of development in which RA may specifically regulate position of pectoral fin progenitors is unknown but long durations of RA deficiency via inhibition of Aldh1a2 during gastrulation or somitogenesis, prevents pectoral fin progenitors from forming (Gibert et al., 2006; Grandel and Brand, 2011). During mid-late gastrulation, *aldh1a2* and *cyp26a* expression are in proximity to the lateral marginal region, the area fate mapped to give rise to pectoral fin (Keegan et al., 2004; Naylor et al., 2016).

RA acts in part through activation of the t-box gene, *Tbx5,* which is the first gene to be expressed in the progenitor cells that later form the vertebrate forelimb (Begemann and Ingham, 2000; Gibson-Brown et al., 1996; Ruvinsky et al., 2000). Vertebrate embryos deficient for TBX5 fail to form forelimbs (Agarwal et al., 2003; Ahn et al., 2002; Ng et al., 2002; Rallis et al., 2003). TBX5 plays an essential role in the early initiation of the wing bud by promoting an epithelial to mesenchymal transition of the LPM in chick (Gros and Tabin, 2014). In zebrafish, Tbx5a directs the migration of the pectoral fin precursors into the prospective fin bud region (Ahn et al., 2002; Mao et al., 2015).

The Caudal (Cdx) transcription factors are key regulators of AP identity and axial elongation during vertebrate development (reviewed by Deschamps and van Nes, 2005). Zebrafish have three Cdx paralogs, Cdx1a, Cdx1b and Cdx4, with Cdx1b mainly associated with phenotypes related to early endoderm formation (Cheng et al., 2008). CDX2 in mice as well as Cdx4 in zebrafish directly bind to loci associated with factors of the RA signaling pathway such as *cyp26a* (Foley et al., 2019; Paik et al., 2013; Savory et al., 2009). Loss of either Cdx2 in mouse or Cdx4 in zebrafish leads to mis-expression of *cyp26a* and *aldh1a2/*

Raldh2 (De Jong et al., 2010; Savory et al., 2009; Shimizu et al., 2006; Wingert et al., 2007; Young et al., 2009). Patterning defects in the foregut, kidney and nervous system of Cdx-deficient embryos result in part from changes associated with RA signaling (Chang et al., 2016; Kinkel et al., 2008; Wingert et al., 2007).

Cdx factors also bind directly to numerous loci associated with formation of cardiac and hematopoietic lineages (Foley et al., 2019; Paik et al., 2013). In particular, Cdx factors bind directly to *Tbx5* in mouse, and CDX-deficient mice ectopically express *Tbx5* and *Nkx2.5* in the yolk sac (Foley et al., 2019). This ectopic expression appears to come at the expense of hematopoietic gene expression and suggest that in mouse, CDX regulates mesodermal fates between cardiac and hematopoietic lineages (Foley et al., 2019). In zebrafish, Cdx-deficient embryos also ectopically express *tbx5a* (Lengerke et al., 2011). However, the consequence of this expansion is unclear since Cdx-deficient embryos go on to form a normal number of differentiating cardiac cells (Lengerke et al., 2011) .

In this work, we determine that RA and the Cdx transcription factors play a related role in regulation of LPM derivatives such as the pectoral fin field. Increasing levels of RA or Cdx4 during gastrulation results in a rostral shift of the fin field. We also show that Cdx-deficiency leads to a caudal expansion of the fin field that later results in a pectoral fin bud that is increased in size. By examining the early effects of RA and Cdx, we determine that Cdx and RA can each restrict the AP position of the fin field.

2. Results

2.1. Cdx1a and Cdx4 regulate the position of the pectoral fin buds along the AP axis

Cdx factors are known regulators of *hox* genes, which have been implicated in regulating limb position. Loss of *Hoxb5* results in a rostral forelimb shift in mice while mis-regulation of *HOX4/9* genes lead to caudal forelimb shifts in chick (Moreau et al., 2018; Rancourt et al., 1995). To examine whether Cdx factors have an effect on pectoral fin development, we compared wild type embryos with double Cdx1a-deficient and Cdx4-deficient embryos (hereafter referred to as Cdx-deficient embryos) at 36hpf, when the larval pectoral fin buds are clearly visible. We visualized the somites using an antibody against myosin heavy chain (MHC) to establish the relative position of the pectoral fins. The fin buds normally form adjacent to the 2nd and 3rd somite. At this stage, as shown in wild type embryos in a lateral view of the left fin bud, the pectoral fins express *dlx2a* in the apical ectodermal ridge (AER) of the fin bud (Fig. 1A). To examine if AP polarity was established in the fin buds of these embryos, we co-stained for *shh,* whose expression is localized to the posterior fin mesenchyme. In Cdx-deficient embryos, *dlx2a* is noticeably upregulated in the fin AER, and expression is now observed adjacent to somites 3-7 (Fig. 1B). Expression of *shh* is still localized to the posterior fin mesenchyme, and also mildly upregulated, as seen adjacent to somites 6-7 (Fig. 1B). There is a subtle delay in the onset of *shh* expression as we do not detect expression in Cdx-deficient embryos at 32hpf, during which expression is clearly visible in wild type (data not shown). The expression of *tbx5a* was used to visualize the overall size of the fin buds. In Fig. 1E, *tbx5a* expression extends along the AP axis of the wild type fin bud, between somites 2-3, while in Cdx-deficient embryos, *tbx5a* expression begins between somites 3-4 and extends posteriorly to somite 7 (Fig. 1F).

To further demonstrate a role for Cdx factors on pectoral fin bud positioning, we transiently overexpressed *cdx4*. A prior mouse study showed increased levels of CDX1 resulted in reduced forelimbs (Gaunt et al., 2008), so we hypothesized that increased levels of Cdx4 could truncate or reduce the pectoral fin bud during a specific developmental window. We used *Tg[phsp70:cdx4]* embryos previously described in (Skromne et al., 2007), to transiently induce *cdx4* expression throughout the embryo. Heat shock controls (HS controls) were *AB fish that were heat shocked during the same developmental time window as *Tg[phsp70:cdx4]* embryos. Compared to HS controls, which always formed fin buds at the normal position adjacent to somites 2-3 (Fig. 1C, G), induced overexpression of *cdx4* led to a high frequency of embryos that formed fin buds rostral to somite 1. In HS controls, *dlx2a* expression was localized in the AER adjacent to somites 2-3, and *shh* expression was restricted to the posterior fin mesenchyme adjacent to somite 3 in a pattern indistinguishable from wild type (Fig. 1C). In heat shocked induced *Tg[phsp70:cdx4]* embryos, *dlx2a* expression is visible in the AER but noticeably shifted anterior to the level of somite 1 and *shh* expression is localized to the posterior fin bud mesenchyme suggesting that normal fin bud polarity is established (Fig. 1D). As indicated by the white arrowheads in Fig. 1G, HS controls have a normal level of *tbx5a* expression that runs adjacent to somites 2-3. In heat shock-induced *Tg[phsp70:cdx4]* embryos, *tbx5a* expression is shifted rostral to the level of somite 1 but there is no visible effect on the overall size of the fin bud compared to HS controls (Fig. 1H).

In order to determine the optimal window where induced overexpression of *cdx4* results in the highest frequency of rostral fin shifts, we heat shocked *Tg[phsp70:cdx4]* embryos for one hour beginning at 4hpf, 7hpf or 11hpf, prior to when the pectoral fin precursors begin to express *tbx5a*. We then examined the frequency of pectoral fin shifts at 36hpf. Heat shocked-induced overexpression of *cdx4* at 4hpf resulted in a moderate frequency (60%) of fin shifts rostral to somite level 1 (Fig. 1I). The frequency of this phenotype peaked at 7hpf when 91% of heat-shocked embryos later displayed rostrally shifted fins. At 11hpf, only 31% of heat-shocked embryos later displayed rostral fin shifts (Fig. 1I). In a subset of fish, we also observed an asymmetry phenotype, where one fin bud was either reduced in size or missing, (Fig. 1I, gray column). For all following experiments, unless stated otherwise, we induced *cdx4* overexpression at 7hpf which resulted in the greatest frequency of rostral fin shifts while still maintaining relatively normal fin morphology.

2.2. A transient increase in RA during gastrulation is sufficient to shift the AP position of the pectoral fin buds

A combination of rostral fin shifts as well as delayed and shorted fin buds was previously reported in zebrafish with a nonsense mutation in the RA degradation enzyme, Cyp26a (Emoto et al., 2005) that presumably results in increased levels of RA at all stages of development. We further investigated whether a transient increase of RA by reversable inhibition of Cyp26a was sufficient to induce changes in the AP position of the pectoral fin bud without resulting in delayed or shortened fin buds. Zebrafish *cyp26a* is first expressed during gastrulation at the blastoderm margin and dorsal ectoderm at 4hpf. Additional Cyp26 paralogs (*cyp26b1* and *cyp26c1*) are only expressed in segments of the hindbrain and not until after gastrulation (Gu et al., 2005; Hernandez et al., 2006; Kudoh et al., 2002; Zhao et

al., 2005). We inhibited Cyp26a activity by treating embryos during a short developmental window with a pan Cyp26 inhibitor called Talarozole (also referred to as R115866) that was previously shown to phenocopy loss of Cyp26 activity in the zebrafish and mouse embryos (Anbalagan et al., 2018; Hernandez et al., 2006; Laue et al., 2008). We then characterized the AP position of the pectoral fin buds in Talarozole-treated embryos compared to controls at 36hpf. In DMSO-treated controls at 36hpf (Fig. 2A, 2C), the left pectoral fin bud forms at the level of somites 2-3 (somites are labeled brown and somite 3 is indicated) (Grandel and Schulte-Merker, 1998). In Talarozole-treated embryos, the fin buds are shifted rostral to somite 1 (Fig. 2B, 2D somite 1 is indicated). Based on the expression of *tbx5a*, used to visualize the whole fin bud mesenchyme, the pectoral fin bud is comparable in size with that of DMSO-treated controls. We examined the AP polarity of these fin buds using expression of *shh* in the posterior fin mesenchyme. In DMSO-treated controls, *shh* expression is restricted to the posterior fin region, as expected (Fig. 2A). The expression of *dlx2a* is also shown, which marks the fin bud anterior ectodermal ridge (AER) and facilitates visualization of *shh* expression relative to the whole fin bud. The pectoral fin buds in Talarozole-treated fish also express *shh* in the posterior fin mesenchyme, however, the area of expression is significantly expanded in these embryos (Fig. 2B). A similar expansion of *shh* expression was previously reported in embryos exposed to excess RA for longer periods of time (Akimenko, M A; Ekker, 1995; Emoto et al., 2005). Expression of *dlx2a* was also upregulated in Talarozole-treated embryos (Fig. 2B).

We did not observe any obvious defects associated with somitogenesis. Related to this, a previous study showed that somitogenesis occurs normally in RA deficient zebrafish (Berenguer et al., 2018). However, in Talarozole-treated fish, we did sometimes observe ectopic expression of expression of Myosin anterior to the first somite that extended towards the shifted fin bud (asterisk, Fig. 2D); these ectopic myosin-expressing cells could represent somitic mesoderm migrating towards the mis-placed fin bud (Talbot et al., 2019).

In order to identify when increased RA had the strongest effect on AP position of the pectoral fins, we examined the frequency of rostral fin shifts that result from applying Talarozole to embryos for one hour beginning at either 4hpf, 7hpf or 11hpf (Fig. 2E, orange columns). These stages were selected to encompass the time between the onset of *cyp26a* expression and the stage where the pectoral fin field is first visible by gene expression. Compared to DMSO-treated controls which all form pectoral fins at somite levels 2-3, embryos treated with Talarozole beginning at 4hpf results in a fin shift rostral to somite 1 in 90% of treated embryos (Fig. 2E). Compared to DMSO-treated controls at 7hpf, 92% of embryos treated with Talarozole at this stage had rostral fin shifts. Talarozole treatments that began at 11hpf resulted in a significant decline in the frequency of rostral fin shifts (15% of treated embryos). From these findings, we conclude that high levels of RA are sufficient to alter position of the pectoral fin bud during gastrulation. For the subsequent experiments described in this work, we performed one-hour Talarozole treatments beginning at 7hpf.

2.3. Increased cdx4 or RA results in mis-patterning of the anterior LPM

In order to examine whether Cdx4 and RA were having identical effects earlier in development, we compared gene expression in the aLPM in Talarozole-treated and heat-

shocked induced *Tg[phsp70:cdx4]* embryos. We hypothesized that the rostral fin shifts resulted either from changes to where fin precursors were specified or changes to where they migrated after being specified. In the case of the former, we would expect a rostral shift of the fin precursors to affect the early pattern of gene expression in the aLPM. The aLPM contains myocardial, pharyngeal and vascular progenitors, which were previously shown to be sensitive to increased levels of RA (De Jong et al., 2010; Keegan et al., 2005; Rydeen and Waxman, 2014). During gastrulation, *cdx4* is expressed near the lateral marginal zone (LMZ) associated with the fate-mapped location of pectoral fin, blood, and cardiac precursors (Davidson et al., 2003; Keegan et al., 2005, 2004; Naylor et al., 2016). After gastrulation, *cdx4* expression has regressed away from the aLPM, towards the tailbud. At 14hpf, as shown in a dorsal view with the anterior oriented towards the top, in HS controls, the stem cell leukemia gene, *scl-1*, begins to be expressed at the anterior end of the aLPM. Expression of *scl-1* was previously fate mapped to cranial vasculature (Rydeen and Waxman, 2014). Expression of this gene extends caudally down the embryo as two bilateral stripes with a posterior boundary just above the level of the anterior end of the notochord (Fig. 3A). In heat-shocked induced *Tg[phsp70:cdx4]* embryos, *scl-1* expression is observed with an anterior boundary that is similar to HS controls but is noticeably truncated in length at the posterior end (Fig.3 B). Talarozole treatments lead to a similar result at 14hpf as that observed in heat-shocked induced *Tg[phsp70:cdx4]* embryos. In DMSO-treated controls, the overall length of *scl-1* expression is localized to the aLPM in a similar pattern to HS controls (compare Fig. 3C with Fig. 3A), while in Talarozole-treated embryos, the length of *scl-1* expression is severely truncated at the posterior end (Fig. 3D), resembling the effect seen in heat-shocked induced *Tg[phsp70:cdx4]* embryos (Fig. 3B).

To compare the effect of increased RA and Cdx4 on gene expression posterior to *scl-1*, we examined the anterior boundary of *tbx5a* and *hand2* expression, which corresponds to the aLPM where cardiac precursors reside at this stage (Schoenebeck et al., 2007). In HS controls, we observe a noticeable gap between the rostral boundary of *tbx5a* expression in the LPM and the eye (Fig. 3E). This distance is significantly reduced in heat-shocked induced *Tg[phsp70:cdx4]* embryos, as the anterior limit of *tbx5a* expression in the LPM shifts rostrally towards the level of the eye (Fig. 3F). In DMSO-treated embryos, there is also a visible gap between *tbx5a* expression in the LPM and eye, while in Talarozole-treated embryos, there is a large rostral shift in expression of *tbx5a* towards the eye, indicated by the red arrowhead (Fig. 3G-H).

Cyp26-deficient embryos were previously shown to have a rostral shift in *hand2* expression in the aLPM at 14hpf, suggesting that increased RA promotes this shift (Rydeen and Waxman, 2014). We examined the effects of increased Cdx4 levels on *hand2* expression at 14hpf. Expression of *hand2* in the aLPM extends bilaterally along the AP axis similar to *tbx5a* expression. In HS controls, the rostral boundary of *hand2* expression relative to the head is not noticeably different from that of heat-shocked induced *Tg[phsp70:cdx4]* embryos (Fig. 3I-J). In DMSO-treated embryos we did not observe a noticeable effect on *hand2* expression compared to HS controls, however there is a sizable rostral shift of *hand2* expression in Talarozole-treated embryos (red arrowhead in Fig. 3L) relative to DMSO-control embryos.

We quantified the AP length of expression of *scl-1* and *tbx5a* under the above described conditions. In Fig. 3Q, we normalized the length of *scl-1* expression to the trunk width and show that there was a statistically significant reduction in the *scl-1* length between HS controls and heat-shocked induced *Tg[phsp70:cdx4]* embryos (p-value<0.001) as well as between DMSO and Talarozole-treated embryos (p-value<0.0001). We also quantified the shift of *tbx5a* expression relative to the posterior edge of the staining in the eye, as shown in Fig. 3R. The distance between the LPM and eye staining is significantly reduced between HS controls and heat-shocked induced *Tg[phsp70:cdx4]* embryos (p-value<0.05) as well as between DMSO and Talarozole-treated embryos (p-value<0.0001).

In order to specifically examine the pectoral fin precursors, we characterized expression of *tbx5a* in the pLPM at 18hpf. Initially, *tbx5a* is expressed as a continuous stripe within the LPM, where it marks fin and other progenitors. At 15ss, the LPM that expresses *tbx5a* separates to form anterior and posterior halves (Ahn et al., 2002; Begemann and Ingham, 2000). By 18hpf, the anterior half has migrated rostrally and the posterior half now flanks somites1-4. This posterior half corresponds to the pectoral fin precursors (Mao et al., 2015; Wyngaarden et al., 2010). We examined the posterior expression of *tbx5a* at 18hpf, by counterstaining for the position of the somites using an antibody for Myosin Heavy Chain protein. As shown in (Fig. 3M), in HS controls, *tbx5a* expression is observed just rostral to the level of somite 1 and extends caudally, just below the level of somite 4. This matches the expression pattern we observe in wild type embryos (Fig. 4I). In heat-shocked induced *Tg[phsp70:cdx4]* embryos, the expression of *tbx5a* is shifted rostrally, with the posterior boundary now positioned adjacent to the level of somite 1 (Fig. 3N). DMSO-treated controls also show a wild type pattern of expression where *tbx5a* flanks somites 1-4 (Fig. 3O). Meanwhile, Talarozole-treated embryos also display a rostral shift in *tbx5a* expression, where the posterior boundary of expression is at the level of somites 1-2 (Fig. 3P). Taken together, these findings show that transiently increasing either Cdx4 or RA in the embryo can result in a rostral shift of the *tbx5a*-expressing fin field relative to both the eye and somites as well as a reduction in length of *scl-1* expression in the adjacent aLPM.

2.4. Cdx-deficient embryos have patterning defects in the pLPM

We were interested in examining whether the caudal shift or the expanded size of the pectoral fin in Cdx-deficient embryos (Fig. 1B, F) were also associated with patterning defects in the LPM. To facilitate this, we first compared gene expression in the aLPM as we did in Figure 3. In wild type, *scl-1* expression begins in the LPM near the head region and extends towards the posterior (Fig. 4A). In Cdx-deficient embryos, *scl-1* expression is located more medially and is disordered. However, the overall length along the AP axis is comparable with wild type embryos (Fig. 4B). We quantified the length of *scl-1* expression (as in Fig. 3Q) and observed a non-significant difference (NS) in length between wild type and Cdx-deficient embryos (p-value>.05, Fig. 4C).

We also examined the anterior boundary of *tbx5a* expression in the aLPM relative to the eye. The distance between *tbx5a* expression in posterior eye and the aLPM of wild type (bracket in Fig. 4D) was not visibly different from that of Cdx-deficient embryos (Fig. 4D-E). We

quantified this distance in Fig. 4F and saw no significant difference between wild type and Cdx-deficient embryos (p-value>.05, NS).

Previously, the pLPM at the level of somite 5 that is posterior to the expression of *tbx5a*, was fate-mapped to the peritoneum (Mao et al., 2015). This region of the LPM expresses *hand2*, which partially overlaps with *tbx5a* expression and extends further posterior in the LPM. We examined *hand2* expression in the pLPM. In wild type embryos that are oriented laterally, *hand2* expression extends along the posterior LPM towards the tailbud region (Fig. 4G). In Cdx-deficient embryos, *hand2* expression is noticeably reduced in length to a faint area of expression near the tailbud region (Fig. 4H).

To specifically examine the AP position of the fin field, we compared expression of *tbx5a* in the LPM between wild type and Cdx-deficient embryos at 18hpf. In wild type embryos, *tbx5a* expression extends from the level just rostral to somite 1 to the level of somite 4 (white arrowheads, Fig. 4I). In Cdx-deficient fish, the anterior limit of *tbx5a* expression begins rostral to the level of somite 1, similar to wild type, however, the posterior boundary of *tbx5a* expression is caudally expanded to the level of somite 7-8 (black arrowheads, Fig. 4J).

Between 18-24hpf, the Tbx5a-positive cells of the fin field converge along the AP axis to where the pectoral fin bud eventually forms. This convergence process requires an Fgf24 signal in order to direct the migration of these fin progenitors into the pectoral fin bud (Fischer et al., 2003; Mao et al., 2015). We compared expression of *fgf24* between wild type and Cdx-deficient embryos at 18hpf. In wild type, we observe expression at the level of somites 2-3 (Fig. 4K). In Cdx-deficient embryos, expression also begins at somite level 2 and extends posteriorly to somite level 4 (Fig. 4L).

2.5. A sub-population of Tbx5a-positive cells fails to migrate from the pLPM to the pectoral fin bud in Cdx-deficient embryos

In wild type embryos, the expression of *tbx5a* in the LPM is a reliable marker for the fin field at 18hpf. To confirm whether changes to *tbx5a* expression in Talarozole-treated embryos accurately reflected the position of the fin field, we characterized the actual population of cells that migrate into the pectoral fin bud by backtracking the movements from time lapse videos of cells that resided at the anterior and posterior ends of the fin bud at 24hpf to the location in the LPM from which they originated at 18hpf. For these experiments, *Tg(tbx5a:eGFP)* fish, which were previously shown to recapitulate endogenous *tbx5a* expression were crossed to *Tg(h2afx:h2afv-mCherry)mw3* fish to allow us to observe the movements of the nuclei of *tbx5a* expressing cells. In Figure 5, the left sides of double transgenic embryos are shown as maximum intensity projections (MIP) post migration at 24hpf (Fig. 5A-H) and at the onset of migration at 18hpf (Fig. 5I-L). GFP-positive cells that migrated into the fin bud by 24hpf are shown in (Fig. 5A-D) and the nuclei of these cells are shown in (Fig. 5E-L).

In DMSO-treated controls, we backtracked 47 cells within the fin bud to the LPM between somite levels 1-4. In addition, a small fraction was observed to have derived from the region rostral to the first somite (Fig. 5M). In Talarozole-treated embryos, the entire fin bud region

was located rostral to somite 1 (Fig. 5B, F) and of the backtracked 58 cells, 50 of these cells originated from the 18 hpf LPM rostral to somite 1, while 8 cells migrated from the level of somite 1. Cells from the LPM at somite levels 2-4, which did not express *tbx5a* (Fig. 3P) in Talarozole-treated embryos, never migrated into the fin bud region (Fig. 5M). These results show that in Talarozole-treated embryos, the *tbx5a*-expressing region at 18hpf accurately reflected the population of cells that migrated to form the pectoral fin bud.

Cdx-deficient embryos have a significant expansion of *tbx5a* expression in the pLPM that in a previous study was reported to result from additional pre-cardiac cells (Lengerke et al., 2011). To address whether these ectopic *tbx5a*-expressing cells became cardiac or fin field cells, we again backtracked the movements of cells from both the anterior and posterior ends of the fin bud at 24hpf to their positions in the 18hpf LPM. In control embryos, six cells were back-tracked from the fin bud region to the LPM region rostral to the first somite, and 38 cells were back-tracked from the fin bud region to the LPM between the level of somites 1-4, (Fig. 5N). In Cdx-deficient embryos, cells rostral to somite 1 were never observed to contribute to the pectoral fin bud. In these Cdx-deficient embryos, 53 cells were back-tracked from the fin bud to the LPM between somites 1-6; within these embryos, 22 of these fin bud cells were shown to have derived from somite levels 5 and 6 (Fig. 5N). In contrast, the Tbx5a-positive cells from somite levels 7-8 were never observed to contribute to the pectoral fin bud despite the increased expression of *tbx5a* in the LPM at the level of somite 7-8 in these Cdx-deficient embryos. Therefore, in contrast to Talarozole-treated embryos, it is possible that the expression of *tbx5a* in a Cdx-deficient background at 18hpf (Fig. 4J) may no longer accurately reflect the population of eventual fin bud progenitors.

Although a subset of the Tbx5a-positive cells at 18hpf did not contribute to the fin bud region in Cdx-deficient embryos, the fin bud region was still visibly larger in AP length compared to controls at 24hpf. This difference was quantified by measuring the AP length of the formed fin bud region (Fig. 5O). The average length of the fin bud region in control embryos was 98.3um while in Cdx-deficient embryos the average length was increased to 194.9um (p-value<.01). Meanwhile, the average length of the fin bud region in DMSO-treated embryos was 91.8um comparable to the average length in Talarozole-treated embryos, which was 99.3um (p-value>.05, indicated NS).

2.6. Overexpression of Cdx4 results in different effects on gene expression compared to increased RA

At the tailbud stage (10hpf), we characterized expression of RA associated genes, namely *aldh1a2* and *cyp26a* which are both known to respond to changes in RA levels to mediate feedback responses (Dobbs-McAuliffe et al., 2004; White et al., 2007). We also examined *hoxd4a*, which shows a similar expression pattern to *cyp26a*, directly adjacent to *aldh1a2*, as another example of an RA responsive target gene (Maves and Kimmel, 2005)

As shown in HS controls, a gap between the anterior *aldh1a2* and *ntl* expression boundaries (white bracket in Fig. 6A), is present that is comparable to that of wt (Fig. 7A). This gap is reduced in *Tg[phsp70:cdx4]* heat-shocked embryos (Fig. 6B). We quantified the *aldh1a2* shifts relative to the *ntl* expression and normalized these measurements relative to the diameter of the yolk. As shown in Fig. 6M, this reduction was highly significant (p-

value<.0001) and appears to result from a rostral shift of the boundary of *aldh1a2* relative to *ntl* (Fig. 6A-B).

In DMSO-control embryos, the *aldh1a2* boundary is located in a similar position to HS controls (compare Fig. 6A, C), while in Talarozole-treated fish, the *aldh1a2* expression boundary is shifted caudally, relative to *ntl* (Fig. 6D). These measurements are quantitated in (Fig. 6M) which shows a small, but significant change in this value for Talarozole-treated embryos.

While Cyp26a is key to regulation of RA levels, the *cyp26a* gene is also a very responsive downstream RA target. Changes to RA levels lead to differences in *cyp26a* expression. We examined the AP position of *cyp26a* in the trunk mesoderm, relative to the posterior boundary of *cyp26a* expression in the neural ectoderm. In HS controls, we observed a visible gap in expression between these regions (white bracket in Fig. 6E). In heat-shocked induced *Tg[phsp70:cdx4]* embryos, we observed the same *cyp26a* expression pattern (Fig. 6 E-F). We quantified the length between *cyp26a* expression in the trunk mesoderm and neuroectoderm, normalized to the diameter of the yolk, and saw no statistically significant difference (p-value>.05 in Fig. 6N). We also observed that compared to DMSO-treated embryos, the expression of *cyp26a* in trunk mesoderm significantly shifts rostrally towards the neuroectoderm in Talarozole-treated embryos (yellow arrowhead in Fig. 6H). The distance between *cyp26a* in the trunk mesoderm and neuroectoderm is significantly reduced, as shown in Fig. 6N (p<.0001). Together, these results show that increased *cdx4* has effects on RA genes that are distinct from the expression pattern when RA levels are increased.

Hoxd4a expression initiates shortly after the tailbud stage (10 hpf) anterior to where *aldh1a2* is expressed (Maves and Kimmel, 2005; Punnamoottil et al., 2008). In HS controls there is a gap between the anterior *hoxd4a* expression limit relative to the anterior tip of the notochord (Fig. 6I). In heat-shocked induced *Tg[phsp70:cdx4]* embryos, *hoxd4a* expression shifts rostrally, closer to the end of the notochord (yellow arrowhead in Fig. 6J). We observe a similar rostral shift in *hoxd4a* when we compare expression between DMSO and Talarozole-treated fish (yellow arrowhead in Fig. 6L). These results are consistent with previous findings that show *hoxd4a* is mis-expressed due to changes in either RA or Cdx4 (Hayward et al., 2015; Maves and Kimmel, 2005)

2.7. Cdx-deficiency results in a caudal shift in aldh1a2 expression

We compared gene expression between wt and Cdx-deficient embryos using the same marker genes examined in Figure 6, namely *aldh1a2, ntl, cyp26a and hoxd4*. As previously mentioned, a prior study fate-mapped the pectoral fins to a region adjacent to where *aldh1a2* is expressed during gastrulation (Naylor et al., 2016). We therefore examined the *aldh1a2* boundary as we did in Figure 6. In wt embryos, viewed dorsally, a gap between the anterior limit of *aldh1a2* and *ntl* expression is present (white bracket in Fig. 7A). This gap was increased in Cdx-deficient embryos, a result of the *aldh1a2* boundary shifting posteriorly (Fig. 7B, black arrowhead). We quantified and compared these length measurements in Cdx-deficient embryos and observed a small but significant increase relative to the anterior boundary of the notochord (Fig. 7G, p<.05). We examined expression of *cyp26a* and *hoxd4a*, both are normally expressed directly anterior to *aldh1a2* (Dobbs-McAuliffe et al.,

2004; Maves and Kimmel, 2005). We compared the trunk expression of *cyp26a* relative to expression in the neural ectoderm and saw no change (Fig. 7C, D, white brackets). We quantified the length between expression in the trunk and neuroectoderm, normalized to the diameter of the yolk and saw no significant difference ($p>.05$, Fig. 7H). While the anterior boundary of *cyp26a* was unaffected, the posterior boundary of trunk *cyp26a* expression was expanded caudally in Cdx-deficient embryos at this stage (black arrowhead in Fig. 7D). This expansion of *cyp26a* has been well documented at later developmental stages in Cdx-deficient embryos (Chang et al., 2016; Shimizu et al., 2006; Wingert et al., 2007). Compared to wild type at 1-2ss, the expression pattern of *hoxd4a* in Cdx-deficient embryos shows a similar caudal expansion of the posterior *hoxd4a* boundary as exhibited in Cdx-deficient embryos (black arrowhead in Fig. 7F). These results suggest that levels of high RA shift posteriorly in Cdx-deficient embryos and that this is accompanied by a posterior expansion of genes normally expressed more rostrally. These expanded genes reflect the later effects we observe in the pectoral fin field.

3. Discussion

3.1. Gastrulation is a developmental window for studying limb positioning along the A-P axis

RA and Cdx have been proposed to act directly through *Hox* genes in patterning tissues along the AP axis. In agreement with this, deletion of entire Hox paralogue groups results in transformations in segments of the axial skeleton (Lohnes, 2003; Mallo et al., 2010). In addition, intriguing correlations between *Hox* expression and forelimb/hindlimb positioning across different species supports a model where a combination of *Hox* genes also establish position of the limbs (Burke et al., 1995; Cohn et al., 1997; Cohn and Tickle, 1999; Minguillon et al., 2012; Nishimoto et al., 2014). With the exception of mutations in the *Hoxb5* gene, targeted deletion of entire paralogous groups of *Hox* genes in mice has no effect on the AP position or size of the forelimbs (Xu et al., 2013; Xu and Wellik, 2011). Thus, it is still unclear what role specific *Hox* genes play in forelimb position. As an alternative to studying a single HOX paralogue group, we focused on upstream regulators that control multiple paralogous groups. Our goal was to identify a precise window when these regulators could alter fin position. In zebrafish, prolonged depletion or increase in RA levels leads to various pectoral fin malformations such as truncations or duplications. To limit unwanted secondary effects on development, we induced limited increases in RA by treating embryos with Talarozole for brief one-hour intervals. These treatments were sufficient to alter the position of the pectoral fin from somite levels 2-3, to regions rostral to somite 1 (Fig. 2B, D). In contrast to a prior study where complete loss of Cyp26a led to underdeveloped pectoral fins (Emoto et al., 2005), in our study, transient inhibition of Cyp26a with Talarozole does not affect the overall size of the pectoral fin. There was an expansion of *shh* expression in the posterior fin mesenchyme of Talarozole-treated embryos (Fig. 2B) but loss or ectopic expression of *shh* in the anterior fin bud was never observed as had been previously observed in embryos with exposure to higher levels of RA (Akimenko, M.A.; Ekker, 1995).

Our data suggest that the positioning of the pectoral fins is primarily affected during gastrulation. One-hour Talarozole treatments beginning at 4hpf are sufficient to shift the pectoral fins anteriorly (Fig. 2E). The frequency of these shifts reaches over 90% when Talarozole treatments were performed at 4hpf or 7hpf (gastrulation) while treatments at 11hpf (post-gastrulation) led to a significant drop in the frequency of rostral fin shifts to 20%. The presence of RA during this precise developmental window also appears to be critical for allowing the pectoral fin field to form as embryos treated with diethylaminobenzaldehyde (an inhibitor of RA synthesis) for one-hour beginning at 7hpf is sufficient to block pectoral fin development (data not shown). Studies suggest gastrulation is also a critical window when RA is required for the limb field to form in other organisms (Moreau et al., 2018). Early RA supplementation during embryonic day 8 (immediately after gastrulation) can also rescue the loss of *Tbx5* expression in the limb field of RA deficient mice (Mic et al., 2004). In chick, inhibition of RA signaling between HH stage 4 and stage 8 is sufficient to shift *tbx5a* expression in the LPM caudally by 2 somites (Mic et al., 2004; Moreau et al., 2018). We also show that transient overexpression of *cdx4* alters pectoral fin position (Fig. 1C, D, G, H). This differs from a mouse study where increased levels of CDX1 led to reduced and underdeveloped forelimbs (Gaunt et al., 2008). These transgenic mice overexpressed *Cdx1* continuously, so these phenotypes likely resulted in part from abnormalities that arose during outgrowth. In this study, we showed that overexpression of *cdx4* for one hour beginning at 7hpf led to a majority of zebrafish embryos with rostral pectoral fin shifts (Fig. 1I). In these embryos, the gene expression patterns of *shh* and *tbx5a* were both unchanged relative to HS controls, which suggests that these fin buds were normal in size and polarity (Fig. 1C, D, G, H). The lack of patterning and outgrowth related phenotypes such as underdeveloped fins suggest that limited overexpression during this developmental stage primarily effects positioning of the limb field and does not result in later developmental effects.

Overall, we have developed a novel approach for studying limb position. Limiting potential downstream candidates of RA and CDX based on the described developmental window will be informative in advancing the understanding of which additional factors contribute to limb/fin positioning. We note that there is additional evidence for a later developmental window when limb positioning can be altered. For example, in chick, the CUX1/2 pair of transcription factors act to refine the position of the limb field at HH stage 13, which is post-gastrulation (Ueda et al., 2019). In the future, it would be interesting to determine if this second window also plays a role in teleost fin positioning.

3.2. tbx5a expression relative to numerous landmarks suggests that the fin field can be shifted more anteriorly

Previously, in Mao et al., 2015, single cell labeling methods identified the area of the lateral plate mesoderm (LPM) adjacent to somite regions 1-4 (s1-4) as giving rise to the mesenchymal portion of the later forming pectoral fin bud. Importantly, it has also been shown in a number of publications (Ahn et al., 2002; Fischer et al., 2003; Mao et al., 2015; Wyngaarden et al., 2010; Yelon et al., 2000) that the early expression of either *hand2* or *tbx5a* within the LPM adjacent to s1-4 overlapped with the fate-mapped LPM cells that will become the fin bud and therefore are reliable markers for the fin field cells in wt zebrafish

embryos. We characterized the expression of *tbx5a* relative to multiple embryonic landmarks as a useful read out of the effects of increased RA and Cdx4 upon fin field position. As shown in Figure 3, we characterized the expression of *tbx5a* relative to the somites. In zebrafish, somite formation has been shown to progress normally in RA-deficient embryos, and in Cyp26a mutants, somite related defects weren't reported, suggesting that the relative shifts we observe are not due to somite abnormalities (Berenguer et al., 2018). In addition, whereas Cdx4 mutants do form much smaller sized posterior somites, the anterior somites, which we use in assessing fin position, are not significantly size altered relative to wt embryos (Davidson et al., 2003). We observed that the fin field, which normally resides adjacent to somites 1-4, now shifts to a position located anteriorly to somite 1 in both Talarozole-treated and heat-shocked induced *Tg[phsp70:cdx4]* embryos at 18hpf as shown in (Fig. 3M-P).

RA has been implicated in eye morphogenesis but the AP position of the eye was unaffected in compound RALDH mutants (Mic et al., 2002; Molotkov et al., 2006). In zebrafish, high concentrations of exogenous RA treatment lead to duplications of the lens along the DV axis but have no reported effects along the AP axis (Hyatt et al., 1992). Therefore, we used the eye, as a landmark to examine the relative shift of the anterior boundary of LPM that expresses *tbx5a*. At 14hpf, the anterior boundary of *tbx5a* expression shifts rostrally, closer to the eye in both Talarozole-treated and heat-shocked induced *Tg[phsp70:cdx4]* embryos (Fig. 3E-H). Quantification of these shifts relative to the eye in Fig. 3R showed more statistically significant differences in Talarozole-treated compared to heat-shocked induced *Tg[phsp70:cdx4]* embryos, ($p<.001$ vs $<.05$).

We also used expression of *ntl* in the notochord as a landmark for comparing gene expression at the tailbud and 1-2ss stages. In Raldh2 mutants, the anterior boundary of the notochord appears unchanged as *ntl* expression extends just anterior to the level of rhombomere 4 as in wt (Grandel et al., 2002). In Cyp26a mutants and embryos treated with excess RA, reduced levels of *ntl* expression are only seen in the posterior tailbud region while expression in the notochord is not affected (Emoto et al., 2005; Martin and Kimelman, 2010). When we examine gene expression post-gastrulation, we see anterior shifts in the RA and Cdx target gene *hoxd4a* relative to the notochord in both Talarozole-treated and heat-shocked induced *Tg[phsp70:cdx4]* embryos (Fig. 6I-L). These expression patterns correlate with the anterior *tbx5a* shifts we later observe in the LPM at 14hpf (Fig. 3E-H) and 18hpf (Fig. 3M-P).

We cannot rule out the possibility of subtle effects to any of our landmarks, but the consistent shifts in gene expression that we observe relative to all three landmarks beginning at the tailbud stage suggests that the AP position of the fin field has already been altered. We show the presumptive location of the fin field at the tailbud stage in Fig. 6O, directly lateral to the AP position where *cyp26a* is expressed. In controls, the fin field extends posteriorly along this region of low RA to the boundary between *cyp26a* and *aldh1a2* expression, where the levels of RA transition from low to high. In Talarozole-treated embryos, the levels of high RA accumulate in the more rostral region where *Cyp26a* would normally be active. Further rostral, away from the *aldh1a2* expression, the levels of high RA eventually drop to low levels where the shifted fin field forms.

The effects on the early fin field and *tbx5a* expression that we observe relative to adjacent landmarks are further corroborated by the effects on gene expression in the LPM rostral to the fin field. Accompanying the anterior shift of *tbx5a* at 14hpf in (Fig. 3E-H), we observe that the length of *scl-1* expression is significantly reduced in both heat-shocked induced *Tg[phsp70:cdx4]* and Talarozole-treated embryos (Fig. 3A-D). Cranial vascular precursors were previously fate mapped to this anterior *scl-1* region and Cyp26a/c double-deficient embryos have a reduced number of cranial vascular progenitors (Rydeen and Waxman, 2014). This suggests that in Talarozole-treated and heat-shocked induced *Tg[phsp70:cdx4]* embryos, the entire LPM is not simply shifting anteriorly but subsets of LPM derivatives are being re-positioned, possibly at the expense of cranial vascular progenitors, supporting an interpretation that the position of the fin field is altered. Together, the use of landmarks and the expression patterns of genes as readouts for how the aLPM is affected by increases in RA and Cdx4, suggest that the AP position of *tbx5a* expression is affected in the early embryo and correlates with the later anterior shift in the location of the pectoral fin buds.

3.3. Cdx1a and Cdx4 are required for normal patterning and migration of the pLPM.

In zebrafish, Cdx-deficient embryos fail to properly pattern the endoderm, as well as the neural ectoderm (Kinkel et al., 2008; Shimizu et al., 2006; Skromne et al., 2007). In mice, loss of *Cdx* genes lead to ectopic expression of numerous cardiac associated genes, suggesting *Cdx* genes may play a role in the general patterning near the limb field region (Lengerke et al., 2011). In Cdx-deficient zebrafish embryos, we observe that the anterior boundary of the pectoral fin buds is shifted caudally by a somite level, whereas the posterior boundary of the pectoral fin buds significantly expands caudally to the level of somite 6 (Fig. 1A-B, E-F), revealing a size phenotype we do not observe when Cdx4 is over-expressed (Fig. 1C-D, G-H).

To examine possible patterning defects related to pectoral fin development, we characterized gene expression patterns in Cdx-deficient embryos prior to the migration of LPM cells into the fin bud. As shown in Figure 4, the anterior boundary of *tbx5a* expression was not changed along the AP axis, relative to the eye or the somites (Fig. 4D-F, K-L) in Cdx-deficient embryos, while the expression length of *scl-1* rostral to *tbx5a* was also unaffected (Fig. 4A-C). This was surprising, given the caudal shift in the positioning of the fin bud we later observed in Cdx-deficient embryos. In contrast, at 18hpf, the posterior *tbx5a* expression boundary is visibly expanded caudally along the LPM from the level of somite 4 to that of somites 7-8 (Fig. 4I, J). At this stage, *hand2* expression normally regresses posteriorly, overlapping partially with *tbx5a* at the level of somites 3-4 but extending further posterior in wt embryos (Fig. 4G). In Cdx-deficient embryos, the expression of *hand2* is not visible in pLPM (Fig. 4 H), including the pLPM region where we see ectopic *tbx5a* (Fig. 4J). Previous fate-mapping of the pLPM adjacent to somite level 4 in (Mao et al., 2015) suggests this region is associated with cells that later contribute to the peritoneum. Identification of reliable genetic markers for this tissue will allow for future characterization of patterning defects associated with the peritoneum.

Although the expression of *tbx5a* in the pLPM normally reflects the cells that migrate into the pectoral fin bud, we examined if this was the case in Cdx-deficient embryos. In a prior

study (Mao et al., 2015), it was shown that the *tbx5a* expressing LPM cells adjacent to somites 1-4, normally converge towards a more centrally located region within the pectoral fin field, such that the definitive wt fin bud became located lateral to somites 2-3. This convergence movement was also shown to be topological, such that pre-migration, rostrally-positioned LPM cells became located in the anterior region of the fin bud, whereas more caudally-positioned LPM cells formed the posterior regions of fin bud. We confocal live imaged GFP expressing cells in the *Tg(tbx5a:GFP)* line and backtracked the migration pathways of cells from both the anterior and posterior pectoral fin bud regions. We confirm findings from previous authors (Ahn et al., 2002; Mao et al., 2015; Wyngaarden et al., 2010) that in wt embryos, LPM cells at the level of somites 1-4 contribute to the fin bud (Fig. 5N). This matches the expression of *tbx5a* we see in (Fig. 4I). In Cdx-deficient embryos, we reliably observe *tbx5a* expression between somite levels 1-7 (Fig. 4J). However, in 3 of out 6 Cdx-deficient embryos that were backtrack analyzed, LPM cells adjacent to somite 1 did not migrate into the fin bud region. Similarly, we never observed cells at the level of somites 7-8 contributing to the fin bud in Cdx-deficient embryos (Fig. 5N). Therefore, in Cdx-deficient embryos, the fin bud mesenchyme was mainly derived from LPM cells adjacent to somite levels 2-6, even though *tbx5a* was expressed at somite levels 1-8 of the pLPM.

The above results suggest that although *tbx5a* expression is expanded in Cdx-deficient embryos, that expression may not now correspond to the entire fin field region. Alternatively, the proper migration of a subset of the fin field into the fin bud may be compromised in Cdx-deficient embryos. In support of the latter, (Mao et al., 2015) previously described partial knock-down phenotypes in which specific subpopulations of LPM cells were unable to migrate into the pectoral fin bud. Fgf24 has been proposed to act as a chemoattractant that directs the surrounding fin field cells to undergo a convergence-type of migration to form the pectoral fin bud, and in embryos deficient in *fgf24*, the *tbx5a*-expressing fin field cells fail to converge to form the fin bud in a manner similar to Tbx5a-deficient and *tbx5a* mutant zebrafish embryos (Ahn et al., 2002; Fischer et al., 2003; Garrity et al., 2002; Mao et al., 2015). In partial loss of either Tbx5a or Fgf24 function through the delivery of sub-optimal dosages of morpholinos, the anterior fin field cells specifically failed to migrate into the fin bud (Mao et al., 2015). Partial knock-down of Fgf24, either directly or indirectly through manipulation of Tbx5a function, was shown to preferentially affect the ability of the most anterior fin field cells to contribute to the fin bud. In Cdx-deficient fish, *fgf24* is expressed within the level of somites 2-6 (Fig. 4K-L). This would place some of the *tbx5a*-expressing LPM cells in Cdx-deficient embryos outside of the region of *fgf24* expression suggesting that the cells adjacent to somite level 1 and 7/8 were either not specified as fin field cells despite *tbx5a* expression or were unable to respond sufficiently to the convergence signal to allow their migration into the forming fin bud. These results suggest that the zebrafish fin field may be confined to a maximal four somite length region of the LPM given constraints upon parameters such as speed of cell migration and diffusion of signaling molecules but that this LPM fin field region can be re-positioned to different AP locations along the body axis.

In contrast to Cdx-deficient embryos, there is no indication that the migration of the fin field in Talarozole-treated embryos is compromised, as the cells that contribute to the pectoral fin bud originate from the region near the level of somite 1 (Fig. 5M), which matches the

expression pattern of *tbx5a* we observe in Fig. 3O-P. This suggests that while the tbx5a-expressing fin field is initially shifted rostrally in Talarozole-treated embryos, all cells within the fin field migrate along its entire length from 18hpf-24hpf to contribute to the fin bud.

3.4. Cdx paralogs and RA act in parallel to restrict AP position of the fin field

Prior studies related to development of various tissues have revealed distinct mechanisms through which RA and Cdx paralogs can act. In the neuroectoderm, RA and Cdx4 act antagonistically with one another to properly position the hindbrain-spinal cord transition (Chang et al., 2016). Meanwhile, in the intermediate mesoderm, Cdx paralogs act through the RA pathway to pattern the pronephros into proximal and distal segments (Wingert et al., 2007). In this study, Cdx paralogs are also necessary to promote high levels of RA in the anterior trunk mesoderm (Fig. 7A-B). However, key differences between Talarozole-treated and heat-shocked induced *Tg[phsp70:cdx4]* embryos suggest Cdx4 can also act on the pectoral fin field independently of the RA pathway. A rostral shift in *hand2* expression in the aLPM of Cyp26a+c deficient embryos was previously reported (Rydeen and Waxman, 2014). In this study, we saw a similar rostral shift of *hand2* expression in Talarozole-treated embryos. Meanwhile, we did not see any effect on *hand2* expression in heat-shocked induced *Tg[phsp70:cdx4]* embryos (Fig. 3J), inconsistent with a mechanism where Cdx4 ultimately results in increased RA. Secondly, in Talarozole-treated embryos there is a clear rostral shift in *cyp26a* expression (Fig. 6H, N). Importantly, the *cyp26a* gene is highly responsive to changes in RA. Yet, *cyp26a* was unaffected in heat-shocked induced *Tg[phsp70:cdx4]* embryos (Fig. 6N). This is not in conflict with the caudal expansion of *cyp26a* expression in Cdx-deficient embryos (Fig. 7D). In a prior study, interactions between Cdx4 and RA differed based on spatial context such that RA could repress *cdx4* expression rostral to the hindbrain-spinal cord transition but not caudal to it (Chang et al., 2016; Lee and Skromne, 2014). Lastly, the temporal window in which we observe rostral pectoral fin shifts in heat-shocked induced *Tg[phsp70:cdx4]* embryos argues against a two-step process where Cdx4 only acts through the RA pathway to regulate the pectoral fin field. A late increase in RA, beginning at 11hpf results in a large decline in frequency of pectoral fin shifts to less than 20% (Fig. 2E). Meanwhile, at 11hpf, increased levels of Cdx4 leads to more than 2x the frequency of rostral pectoral fin shifts (40%). This suggests Cdx4 can influence the pectoral fin field past 11hpf when RA is no longer as effective. In a sequential pathway scenario where Cdx4 only acts through RA, we would have expected increased Cdx4 to be less effective than RA at 11hpf. Based on these observations, our summary model (Fig. 8) shows a pathway where Cdx4 can promote RA and then in parallel, RA and Cdx4 can both restrict the fin field. Our model implies that an increase in either Cdx4 (Fig. 8A) or RA (Fig. 8B) is sufficient to alter the position of the pectoral fin field and that RA and Cdx4 could compensate for each other. Although RA is still present to restrict the pectoral fin field in Cdx-deficient embryos, the caudal shift in high levels of RA we observed in these embryos at the tailbud stage (compare *aldh1a2* expression in Fig. 7A-B) would explain the caudal expansion of the fin field at this stage (Fig. 7I and Fig. 8C). An implication of this model is that in the absence of RA, the pectoral fin field boundary would still be established. Prior studies showed the pectoral fin loss in RA deficient fish could be rescued by loss of Fgf signaling (Cunningham et al., 2013; Sorrell and Waxman, 2011; Zhao et al., 2009). The position and size of the fin buds were not described in these embryos. One

predication is that Cdx1a/Cdx4 could still restrict the fin field from expanding further posteriorly.

In conclusion, the molecular mechanisms that determine how forelimbs are precisely positioned along the AP axis are not fully understood. Our study proposes Cdx1a/4 as key upstream regulators of the pectoral fin field and highlights important interactions between Cdx and RA during gastrulation. Our transient mis-regulation of RA and Cdx during a refined developmental window provides a new approach for studying limb placement during development.

4. Materials and Method

4.1. Zebrafish Husbandry, pharmacological treatments, heat shock and microinjection

Zebrafish were raised and maintained using standard protocol. Zebrafish embryos were maintained at 28.5° C in E3 media (5 mM NaCl, 0.17 mM KCL, 0.33 mM CaCl, 0.33 mM $MgSO_4$) and staged as described in (Kimmel et al., 1995). Embryos were collected from crosses between *AB stocks or from previously described transgenic zebrafish lines *Tg(tbx5a:eGFP)* (Ocaña et al. 2017), and (*Tg(h2afx:h2afv-mCherry)mw3* (McMahon et al. 2009). Heat shock overexpression of *cdx4* was performed using *Tg[phsp70:cdx4]* as previously described (Skromne et al. 2007) Microinjection of Cdx1a and Cdx4 morpholinos were performed at the 1 cell stage as previously described using standard protocols (Skromne et al. 2007). Specificity of morpholinos was assessed by comparing embryos injected with anti-cdx or anti-GFP morpholinos. *AB or double transgenics were incubated in 0.1% DMSO in embryo media, 10um diethylaminobenzaldehyde (Aldrich) for one hour beginning at 7hpf, or 10um Talarozole (MedChem Express) for one hour beginning at either, 4hpf, 7hpf or 11hpf.

4.2. In-situ hybridization and immunohistochemistry

Standard in-situ protocol using NBT/BCIP as the substrate was used for gene expression characterization of *aldh1a2* (Begemann et al., 2001) *cdx4* (Skromne et al., 2007); *cyp26a1* (Hernandez et al., 2006) *dlx2a*; (Akimenko, M A; Ekker, 1995) *hoxd4a* (Prince et al., 1998); and *no tail* (Schulte-Merker et al., 1992). Antibody stain was performed using mouse anti-myosin heavy chain at a concentration of 1:100 (A4.1025. Developmental Studies, Hybridoma bank, IA, USA). Anti-mouse IgG (H+L) secondary antibody (Vector laboratories, PI-2000) was used at 1:200 dilution. DAB color development was performed using the Peroxidase Substrate Kit (Vector laboratories, SK-4100).

4.3. Imaging, cell tracking and statistical analysis

Images were collected on a Zeiss compound microscope using a Nikon-5000 camera and compiled using Adobe Illustrator. Measurements were performed using FIJI and statistical significance was determined using the student t-test (* indicates $p<0.05$, ** indicates $p<0.01$, *** indicates $P<0.001$, **** indicates $p<0.0001$). Live imaging was performed on dechorionated embryos at 28.5 C using 0.5% low melting-point agarose (Sigma;A9414) in E3 medium with 0.16% tricane. An upright Zeiss LSM710 confocal microscope with the

Plan-Apochromat 20x/0.8 (working distance:0.5mm) objective was used to collect z-stacks every 8 minutes. Cell tracking was done using the Manual Tracking plugin for FIJI.

Acknowledgements

We would like to thank Adam Kuuspalu for excellent fish care and assistance with confocal microscopy maintenance and operations.

Funding

This work was supported by The National Institutes of Health (R01 HD072598, T32 GM007183, T32 HD055164).

References

Agarwal P, Wylie JN, Galceran J, Arkhitko O, Li C, Deng C, Grosschedl R, Bruneau BG, 2003 Tbx5 is essential for forelimb bud initiation following patterning of the limb field in the mouse embryo. Development 130, 623–33. 10.1242/dev.00191 [PubMed: 12490567]

Ahn DG, Kourakis MJ, Rohde LA, Slivert LM, Ho RK, 2002 T-box gene Tbx5 is essential for formation of the pectoral limb bud. Nature 417, 754–758. 10.1038/nature00814 [PubMed: 12066188]

Akimenko MA; Ekker M, 1995 Anterior Duplication of the Sonic hedgehog Expression Pattern in the Pectoral Fin Buds of Zebrafish Treated with Retinoic Acid. Dev. Biol 10.1006/dbio.1995.1211

Anbalagan S, Gordon L, Blechman J, Matsuoka RL, Rajamannar P, Wircer E, Biran J, Reuveny A, Leshkowitz D, Stainier DYR, Levkowitz G, 2018 Pituicyte Cues Regulate the Development of Permeable Neuro-Vascular Interfaces. Dev. Cell 47, 711–726.e5. 10.1016/j.devcel.2018.10.017 [PubMed: 30449506]

Begemann G, Ingham PW, 2000 Developmental regulation of Tbx5 in zebrafish embryogenesis. Mech. Dev 90, 299–304. 10.1016/S0925-4773(99)00246-4 [PubMed: 10640716]

Begemann G, Schilling TF, Rauch GJ, Geisler R, Ingham PW, 2001 The zebrafish neckless mutation reveals a requirement for raldh2 in mesodermal signals that pattern the hindbrain. Development 128, 3081–94. [PubMed: 11688558]

Berenguer M, Lancman JJ, Cunningham TJ, Dong PDS, Duester G, 2018 Mouse but not zebrafish requires retinoic acid for control of neuromesodermal progenitors and body axis extension. Dev. Biol 441, 127–131. 10.1016/j.ydbio.2018.06.019 [PubMed: 29964026]

Burke AC, Nelson CE, Morgan BA, Tabin C, 1995 Hox genes and the evolution of vertebrate axial morphology. Development 121, 333–46. [PubMed: 7768176]

Chang J, Skromne I, Ho RK, 2016 CDX4 and retinoic acid interact to position the hindbrain-spinal cord transition. Dev. Biol 410, 178–189. 10.1016/j.ydbio.2015.12.025 [PubMed: 26773000]

Cheng P-Y, Lin C-C, Wu C-S, Lu Y-F, Lin CY, Chung C-C, Chu C-Y, Huang C-J, Tsai C-Y, Korzh S, Wu J-L, Hwang S-PL, 2008 Zebrafish cdx1b regulates expression of downstream factors of Nodal signaling during early endoderm formation. Development 135, 941–952. 10.1242/dev.010595 [PubMed: 18234726]

Cohn MJ, Patel K, Krumlauf R, Wilkinsont DG, Clarke JDW, Tickle C, 1997 Hox9 genes and vertebrate limb specification. Nature 387, 97–101. 10.1038/387097a0 [PubMed: 9139829]

Cohn MJ, Tickle C, 1999 Developmental basis of limblessness and axial patterning in snakes anterior posterior 399 10.1038/20944

Cunningham TJ, Duester G, 2015 Mechanisms of retinoic acid signalling and its roles in organ and limb development. Nat. Rev. Mol. Cell Biol 16, 110–123. 10.1038/nrm3932 [PubMed: 25560970]

Cunningham TJ, Zhao X, Sandell LL, Evans SM, Trainor PA, Duester G, 2013 Antagonism between Retinoic Acid and Fibroblast Growth Factor Signaling during Fimb Development. Cell Rep. 3, 1503–1511. 10.1016/j.celrep.2013.03.036 [PubMed: 23623500]

Davidson AJ, Ernst P, Wang Y, Dekens MPS, Kingsley PD, Palis J, Korsmeyer SJ, Daley GQ, Zon LI, 2003 Cdx4 Mutants Fail To Specify Blood Progenitors and Can Be Rescued By Multiple Hox Genes. Nature 425, 300–306. 10.1038/nature01973 [PubMed: 13679919]

De Jong JLO, Davidson AJ, Wang Y, Palis J, Opara P, Pugach E, Daley GQ, Zon LI, 2010 Interaction of retinoic acid and scl controls primitive blood development. Blood 116, 201–209. 10.1182/blood-2009-10-249557 [PubMed: 20410509]

Deschamps J, van Nes J, 2005 Developmental regulation of the Hox genes during axial morphogenesis in the mouse. Development 132, 2931–2942. 10.1242/dev.01897 [PubMed: 15944185]

Dobbs-McAuliffe B, Zhao Q, Linney E, 2004 Feedback mechanisms regulate retinoic acid production and degradation in the zebrafish embryo. Mech. Dev 121, 339–350. 10.1016/j.mod.2004.02.008 [PubMed: 15110044]

Duester G, 2008 Retinoic Acid Synthesis and Signaling during Early Organogenesis. Cell 134, 921–931. 10.1016/j.cell.2008.09.002 [PubMed: 18805086]

Emoto Y, Wada H, Okamoto H, Kudo A, Imai Y, 2005 Retinoic acid-metabolizing enzyme Cyp26a1 is essential for determining territories of hindbrain and spinal cord in zebrafish. Dev. Biol 278, 415–427. 10.1016/j.ydbio.2004.11.023 [PubMed: 15680360]

Fischer S, Draper BW, Neumann CJ, 2003 The zebrafish fgf24 mutant identifies and additional level of Fgf signaling involved in vertebrate forelimb initiation. Development 130, 3515–3524. 10.1242/dev.00537 [PubMed: 12810598]

Foley TE, Hess B, Savory JGA, Ringuette R, Lohnes D, 2019 Role of Cdx factors in early mesodermal fate decisions. Development 146, dev170498 10.1242/dev.170498 [PubMed: 30936115]

Garrity DM, Childs S, Fishman MC, 2002 The heartstrings mutation in zebrafish causes heart/fin Tbx5 deficiency syndrome. Development 129, 4635–4645. [PubMed: 12223419]

Gaunt SJ, Drage D, Trubshaw RC, 2008 Increased Cdx protein dose effects upon axial patterning in transgenic lines of mice. Development 135, 2511–2520. 10.1242/dev.015909 [PubMed: 18579683]

Gibert Y, Gajewski A, Meyer A, Begemann G, 2006 Induction and prepatterning of the zebrafish pectoral fin bud requires axial retinoic acid signaling. Development 133, 2649–2659. 10.1242/dev.02438 [PubMed: 16774994]

Gibson-Brown JJ, Agulnik SI, Chapman DL, Alexiou M, Garvey N, Silver LM, Papaioannou VE, 1996 Evidence of a role for T-box genes in the evolution of limb morphogenesis and the specification of forelimb/hindlimb identity. Mech. Dev 56, 93–101. 10.1016/0925-4773(96)00514-X [PubMed: 8798150]

Grandel H, Brand M, 2011 Zebrafish limb development is triggered by a retinoic acid signal during gastrulation. Dev. Dyn 240, 1116–1126. 10.1002/dvdy.22461 [PubMed: 21509893]

Grandel H, Lun K, Rauch G-J, Rhinn M, Piotrowski T, Houart C, Sordino P, Küchler AM, Schulte-Merker S, Geisler R, Holder N, Wilson SW, Brand M, 2002 Retinoic acid signalling in the zebrafish embryo is necessary during pre-segmentation stages to pattern the anterior-posterior axis of the CNS and to induce a pectoral fin bud. Development 129, 2851–65. [PubMed: 12050134]

Grandel H, Schulte-Merker S, 1998 The development of the paired fins in the Zebrafish (Danio rerio). Mech. Dev 79, 99–120. [PubMed: 10349624]

Gros J, Tabin J,C, 2014 Vertebrate Limb bud formation is initiated by localized Epithelial to Mesenchymal Transition. Science (80-.). 343, 1253–1256. 10.1126/science.1248228

Gu X, Xu F, Wang X, Gao X, Zhao Q, 2005 Molecular cloning and expression of a novel CYP26 gene (cyp26d1) during zebrafish early development. Gene Expr. Patterns 5, 733–739. 10.1016/j.modgep.2005.04.005 [PubMed: 15979416]

Hayward AG, Joshi P, Skromne I, 2015 Spatiotemporal analysis of zebrafish hox gene regulation by Cdx4. Dev. Dyn 244, 1564–1573. 10.1002/dvdy.24343 [PubMed: 26335559]

Hernandez RE, Putzke AP, Myers JP, Margaretha L, Moens CB, 2006 Cyp26 enzymes generate the retinoic acid response pattern necessary for hindbrain development. Development 134, 177–187. 10.1242/dev.02706

Hyatt GA, Schmitt EA, Marsh-Armstrong NR, Dowling JE, 1992 Retinoic acid-induced duplication of the zebrafish retina. Proc. Natl. Acad. Sci. U. S. A 89, 8293–8297. 10.1073/pnas.89.17.8293 [PubMed: 1518861]

Keegan BR, Feldman JL, Begemann G, Ingham PW, Yelon D, 2005 Retinoic acid signaling restricts the cardiac progenitor pool. Science (80-.). 307, 247–249. 10.1126/science.1101573

Keegan BR, Meyer D, Yelon D, 2004 Organization of cardiac chamber progenitors in the zebrafish blastula. Development 131, 3081–3091. 10.1242/dev.01185 [PubMed: 15175246]

Kimmel CB, Ballard WW, Kimmel SR, Ullmann B, Schilling TF, 1995 Stages of embryonic development of the zebrafish. Dev. Dyn 203, 253–310. 10.1002/aja.1002030302 [PubMed: 8589427]

Kinkel MD, Eames SC, Alonzo MR, Prince VE, 2008 Cdx4 is required in the endoderm to localize the pancreas and limit -cell number. Development 135, 919–929. 10.1242/dev.010660 [PubMed: 18234725]

Kudoh T, Wilson SW, Dawid IB, 2002 Distinct roles for Fgf, Wnt and retinoic acid in posteriorizing the neural ectoderm. Development 129, 4335–46. [PubMed: 12183385]

Laue K, Jänicke M, Plaster N, Sonntag C, Hammerschmidt M, 2008 Restriction of retinoic acid activity by Cyp26b1 is required for proper timing and patterning of osteogenesis during zebrafish development. Development 135, 3775–3787. 10.1242/dev.021238 [PubMed: 18927157]

Lee K, Skromne I, 2014 Retinoic acid regulates size, pattern and alignment of tissues at the head-trunk transition. Development 141, 4375–4384. 10.1242/dev.109603 [PubMed: 25371368]

Lengerke C, Wingert R, Beeretz M, Grauer M, Schmidt AG, Konantz M, Daley GQ, Davidson AJ, 2011 Interactions between Cdx genes and retinoic acid modulate early cardiogenesis. Dev. Biol 354, 134–142. 10.1016/j.ydbio.2011.03.027 [PubMed: 21466798]

Lohnes D, 2003 The Cdx1 homeodomain protein : an integrator of posterior signaling in the mouse. BioEssays 971–980. 10.1002/bies.10340 [PubMed: 14505364]

Mallo M, Wellik DM, Deschamps J, 2010 Hox genes and regional patterning of the vertebrate body plan. Dev. Biol 344, 7–15. 10.1016/j.ydbio.2010.04.024 [PubMed: 20435029]

Mao Q, Stinnett HK, Ho RK, 2015 Asymmetric cell convergence-driven zebrafish fin bud initiation and pre-pattern requires Tbx5a control of a mesenchymal Fgf signal. Development 142, 4329–4339. 10.1242/dev.124750 [PubMed: 26525676]

Martin BL, Kimelman D, 2010 Brachyury establishes the embryonic mesodermal progenitor niche. Genes Dev. 24, 2778–2783. 10.1101/gad.1962910 [PubMed: 21159819]

Maves L, Kimmel CB, 2005 Dynamic and sequential patterning of the zebrafish posterior hindbrain by retinoic acid. Dev. Biol 285, 593–605. 10.1016/j.ydbio.2005.07.015 [PubMed: 16102743]

Mic FA, Haselbeck RJ, Cuenca AE, Duester G, 2002 Novel retinoic acid generating activities in the neural tube and heart identified by conditional rescue of Raldh2 null mutant mice. Development 129, 2271–2282. [PubMed: 11959834]

Mic FA, Sirbu IO, Duester G, 2004 Retinoic acid synthesis controlled by Raldh2 is required early for limb bud initiation and then later as a proximodistal signal during apical ectodermal ridge formation. J. Biol. Chem 279, 26698–26706. 10.1074/jbc.M401920200 [PubMed: 15069081]

Minguillon C, Nishimoto S, Wood S, Vendrell E, Gibson-Brown JJ, Logan MPO, 2012 Hox genes regulate the onset of Tbx5 expression in the forelimb. Development 139, 3180–3188. 10.1242/dev.084814 [PubMed: 22872086]

Molotkov A, Molotkova N, Duester G, 2006 Retinoic acid guides eye morphogenetic movements via paracrine signaling but is unnecessary for retinal dorsoventral patterning. Development 133, 1901–1910. 10.1242/dev.02328 [PubMed: 16611695]

Moreau C, Caldarelli P, Rocancourt D, Roussel J, Denans N, Pourquie O, Gros J, 2018 Timed collinear activation of Hox genes during gastrulation controls the avian forelimb position 1–25. 10.1016/j.cub.2018.11.009

Naylor RW, Skvarca LB, Thisse C, Thisse B, Hukriede NA, Davidson AJ, 2016 BMP and retinoic acid regulate anterior-posterior patterning of the non-axial mesoderm across the dorsal-ventral axis. Nat. Commun 7, 1–14. 10.1038/ncomms12197

Ng JK, Kawakami Y, Büscher D, Raya Á, Itoh T, Koth CM, Rodríguez Esteban C, Rodríguez-León J, Garrity DM, Fishman MC, Belmonte JCI, 2002 The limb gene Tbx5 promotes limb initiation by interacting with Wnt2b adn Fgf10. Development 129, 5161–5170. [PubMed: 12399308]

Nishimoto S, Minguillon C, Wood S, Logan MPO, 2014 A Combination of Activation and Repression by a Colinear Hox Code Controls Forelimb-Restricted Expression of Tbx5 and Reveals Hox Protein Specificity. PLoS Genet. 10, 1–13. 10.1371/journal.pgen.1004245

Paik EJ, Mahony S, White RM, Price EN, Dibiase A, Dorjsuren B, Mosimann C, Davidson AJ, Gifford D, Zon LI, 2013 A Cdx4-sall4 regulatory module controls the transition from mesoderm formation

to embryonic hematopoiesis. Stem Cell Reports 1, 425–436. 10.1016/j.stemcr.2013.10.001 [PubMed: 24286030]

Prince VE, Joly F, Ekker M, Ho RK, 1998 Zebrafish hox genes: Genomic organization and modified colinear expression patterns in the trunk. Development 125, 407–420. [PubMed: 9425136]

Punnamoottil B, Kikuta H, Pezeron G, Erceg J, Becker TS, Rinkwitz S, 2008 Enhancer detection in zebrafish permits the identification of neuronal subtypes that express Hox4 paralogs. Dev. Dyn 237, 2195–2208. 10.1002/dvdy.21618 [PubMed: 18627100]

Rallis C, Bruneau BG, Del Buono J, Seidman CE, Seidman JG, Nissim S, Tabin CJ, Logan MPO, 2003 Tbx5 is required for forelimb bud formation and continued outgrowth. Development 130, 2741–2751. 10.1242/dev.00473 [PubMed: 12736217]

Rancourt DE, Tsuzuki T, Capecchi MR, 1995 Genetic interaction between hoxb-5 and hoxb-6 is revealed by nonallelic noncomplementation. Genes Dev. 9, 108–122. 10.1101/gad.9.1.108 [PubMed: 7828847]

Ruvinsky I, Oates AC, Silver LM, Ho RK, 2000 The evolution of paired appendages in vertebrates: T-box genes in the zebrafish. Dev. Genes Evol 210, 82–91. 10.1007/s004270050014 [PubMed: 10664151]

Rydeen AB, Waxman JS, 2014 Cyp26 enzymes are required to balance the cardiac and vascular lineages within the anterior lateral plate mesoderm. Development 141, 1638–1648. 10.1242/dev.105874 [PubMed: 24667328]

Savory JGA, Bouchard N, Pierre V, Rijli FM, De Repentigny Y, Kothary R, Lohnes D, 2009 Cdx2 regulation of posterior development through non-Hox targets. Development 136, 4099–4110. 10.1242/dev.041582 [PubMed: 19906845]

Schoenebeck JJ, Keegan BR, Yelon D, 2007 Vessel and Blood Specification Override Cardiac Potential in Anterior Mesoderm. Dev. Cell 13, 254–267. 10.1016/j.devcel.2007.05.012 [PubMed: 17681136]

Schulte-Merker S, Ho RK, Herrmann BG, Nusslein-Volhard C, 1992 The protein product of the zebrafish homologue of the mouse T gene is expressed in nuclei of the germ ring and the notochord of the early embryo. Development 116, 1021–1032. [PubMed: 1295726]

Shimizu T, Bae Y-K, Hibi M, 2006 Cdx-Hox code controls competence for responding to Fgfs and retinoic acid in zebrafish neural tissue. Development 133, 4709–4719. 10.1242/dev.02660 [PubMed: 17079270]

Skromne I, Thorsen D, Hale M, Prince VE, Ho RK, 2007 Repression of the hindbrain developmental program by Cdx factors is required for the specification of the vertebrate spinal cord. Development 134, 2147–2158. 10.1242/dev.002980 [PubMed: 17507415]

Sorrell MRJ, Waxman JS, 2011 Restraint of Fgf8 signaling by retinoic acid signaling is required for proper heart and forelimb formation. Dev. Biol 358, 44–55. 10.1016/j.ydbio.2011.07.022 [PubMed: 21803036]

Talbot JC, Teets EM, Ratnayake D, Duy PQ, Currie PD, Amacher SL, 2019 Muscle precursor cell movements in zebrafish are dynamic and require Six family genes. Development 146 10.1242/dev.171421

Ueda S, Cordeiro IR, Moriyama Y, Nishimori C, Kai K, Yu R, Nakato R, Shirahige K, Tanaka M, 2019 Cux2 refines the forelimb field by controlling expression of Raldh2 and Hox genes. Biol. Open 8, 040584 10.1242/bio.040584

Vandersea MW, Fleming P, McCarthy RA, Smith DG, 1998 Fin duplications and deletions induced by disruption of retinoic acid signaling. Dev. Genes Evol 208, 61–68. 10.1007/s004270050155 [PubMed: 9569347]

White RJ, Nie Q, Lander AD, Schilling TF, 2007 Complex regulation of cyp26a1 creates a robust retinoic acid gradient in the zebrafish embryo. PLoS Biol. 5, 2522–2533. 10.1371/journal.pbio.0050304

Wingert RA, Selleck R, Yu J, Song HD, Chen Z, Song A, Zhou Y, Thisse B, Thisse C, McMahon AP, Davidson AJ, 2007 The cdx genes and retinoic acid control the positioning and segmentation of the zebrafish pronephros. PLoS Genet. 3, 1922–1938. 10.1371/journal.pgen.0030189 [PubMed: 17953490]

Wyngaarden LA, Vogeli KM, Ciruna BG, Wells M, Hadjantonakis A-K, Hopyan S, 2010 Oriented cell motility and division underlie early limb bud morphogenesis. J. Cell Sci 123, e1 10.1242/jcs077784

Xu B, Hrycaj SM, McIntyre DC, Baker NC, Takeuchi JK, Jeannotte L, Gaber ZB, Novitch BG, Wellik DM, 2013 Hox5 interacts with Plzf to restrict Shh expression in the developing forelimb. Proc. Natl. Acad. Sci. U. S. A 110, 19438–19443. 10.1073/pnas.1315075110 [PubMed: 24218595]

Xu B, Wellik DM, 2011 Axial Hox9 activity establishes the posterior field in the developing forelimb. Proc. Natl. Acad. Sci 108, 4888–4891. 10.1073/pnas.1018161108 [PubMed: 21383175]

Yelon D, Ticho B, Halpern ME, Ruvinsky I, Ho RK, Silver LM, Stainier DY, 2000 The bHLH transcription factor hand2 plays parallel roles in zebrafish heart and pectoral fin development. Development 127, 2573–82. [PubMed: 10821756]

Young T, Rowland JE, van de Ven C, Bialecka M, Novoa A, Carapuco M, van Nes J, de Graaff W, Duluc I, Freund JN, Beck F, Mallo M, Deschamps J, 2009 Cdx and Hox Genes Differentially Regulate Posterior Axial Growth in Mammalian Embryos. Dev. Cell 17, 516–526. 10.1016/j.devcel.2009.08.010 [PubMed: 19853565]

Zhao Q, Dobbs-McAuliffe B, Linney E, 2005 Expression of cyp26b1 during zebrafish early development. Gene Expr. Patterns 5, 363–369. 10.1016/j.modgep.2004.09.011 [PubMed: 15661642]

Zhao X, Sirbu IO, Mic FA, Molotkova N, Molotkov A, Kumar S, Duester G, 2009 Retinoic Acid Promotes Limb Induction through Effects on Body Axis Extension but Is Unnecessary for Limb Patterning. Curr. Biol 19, 1050–1057. 10.1016/j.cub.2009.04.059 [PubMed: 19464179]

- Zebrafish pectoral fin position is specified by late gastrulation
- Transient over-expression of RA or Cdx4 leads to a rostral mis-positioning of pectoral fins
- Knock-down of *cdx* genes leads to a caudal mis-positioning of pectoral fins.
- RA and Cdx4 act in parallel to regulate the position of pectoral fin progenitors

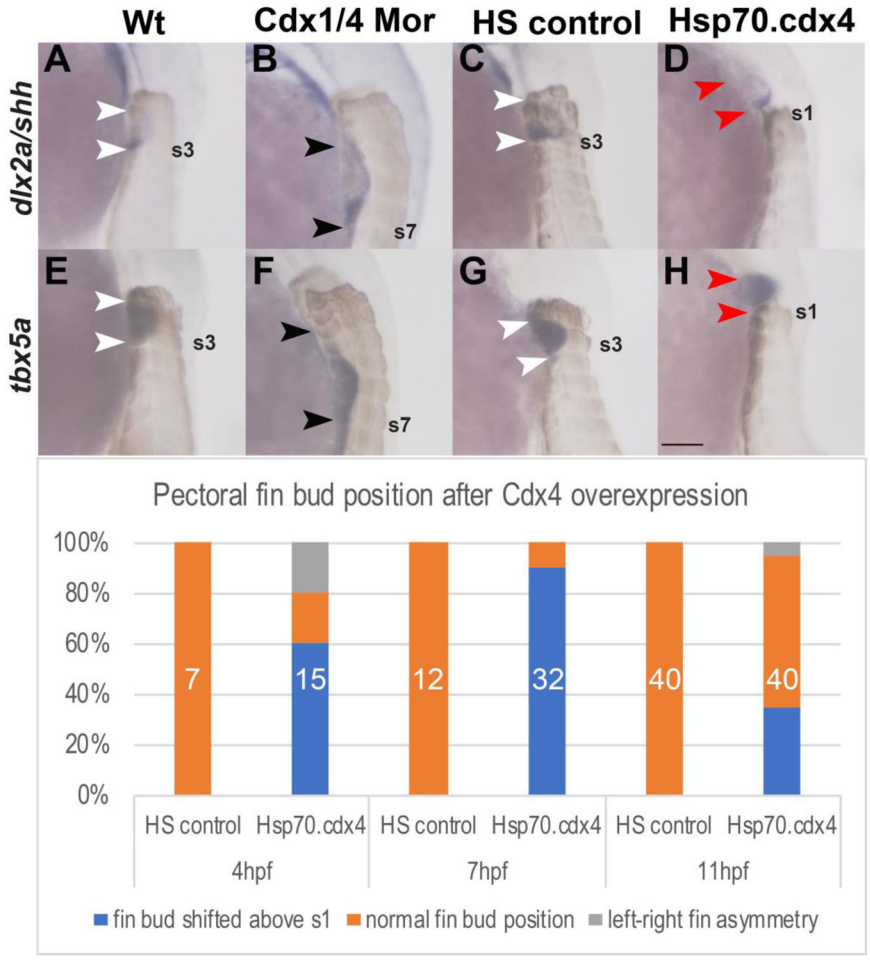

Fig. 1.

Cdx1a and Cdx4 regulate the position and size of the pectoral fin buds along the AP axis. (A-H) In situ hybridizations for the pectoral fin AER marker *dlx2a* (A-D), *shh* (A-D) and *tbx5a* (E-H) in lateral view at 36hpf show caudal shift and expansion of the fin buds (B, F) as well as rostral shift of the pectoral fin bud (D, H) relative to the somites (brown). Fin buds are positioned at the level of somites 2-3 in wt (white arrowheads indicate somite level 2-3, A, E). Pectoral fin buds form at somite level 3-7 in Cdx-deficient embryos (black arrowheads in B, F indicate extent of fin buds that form adjacent to somites 3 and somite 7 (indicated as s7). Pectoral fin buds form at somite levels 2-3 in HS controls (white arrowheads, C, G) while in Hsp70.cdx4 fish, they form rostral to the level of somite 1 (red arrowheads, D, H). (I) The frequency of rostral fin bud shifts after induced *cdx4* overexpression beginning at either 4,7 or 11hpf is indicated as % of total embryos. The corresponding numbers are: 9/15 embryos at 4hpf, 29/32 embryos at 7hpf and 14/40 embryos at 11hpf. Total number of embryos used is indicated in white. Scale bar represents 100um.

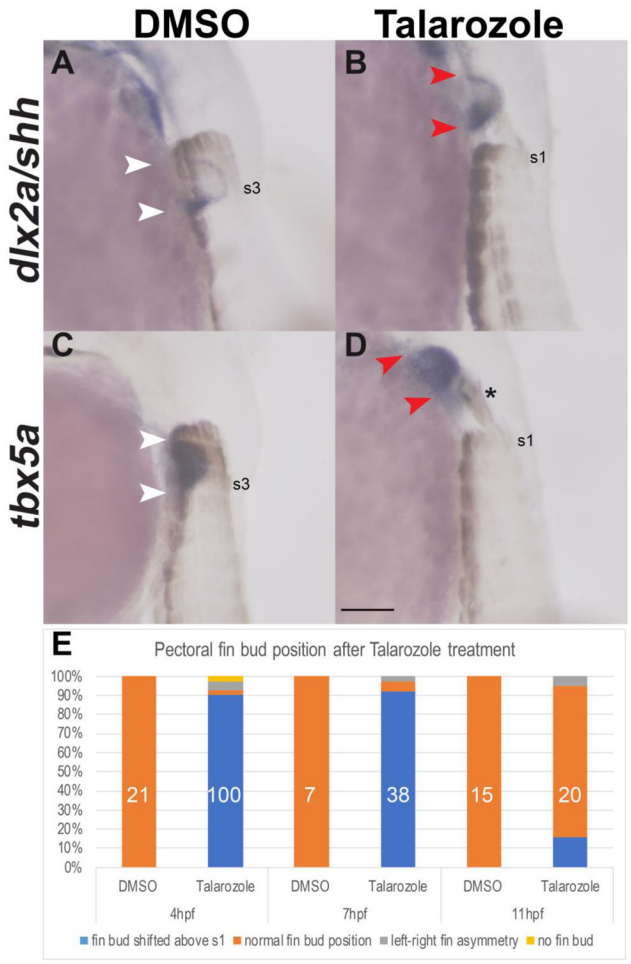

Fig. 2.

Increased levels of RA during gastrulation are sufficient to shift the pectoral fins rostrally. (A-D) In situ hybridization for the pectoral fin markers *dlx2a/shh* (A-B) and *tbx5a* (C-D) in lateral view at 36hpf show rostral fin bud shifts relative to the somites which are marked by Myosin Heavy Chain (ectopic Myosin above s1 indicated by the asterisk). Fin bud forms at the level of somites 2-3 in DMSO-treated controls (white arrowheads in A, C). Pectoral fin buds form rostral to somite level 1 in Talarozole-treated embryos (red arrowheads B, D). Somites 1 or 3 are indicated (s1 and s3, respectively). (E) The frequency of rostral fin shifts at 36 hpf after one hour of Talarozole application beginning at either 4, 7 or 11 hpf is indicated as % of total embryos. The corresponding numbers are: 99/110 embryos at 4hpf, 35/38 embryos at 7hpf and 3/20 embryos at 11hpf. Total number of embryos examined is indicated in white. Scale bar represents 100um.

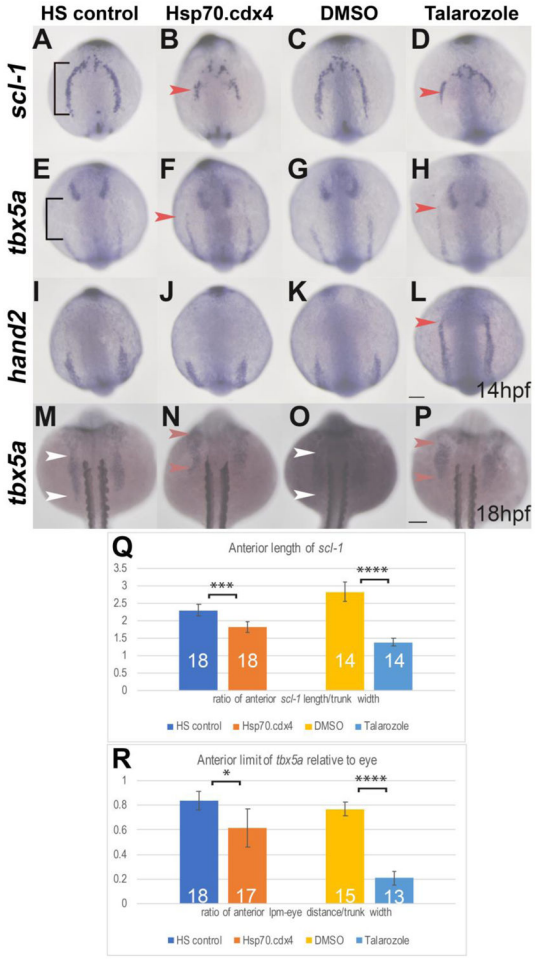

Fig.3.

Increased RA or Cdx4 results in mis-patterning in the anterior LPM. (A-L) In situ hybridization at 14hpf for aLPM markers *scl-1* (A-D), *tbx5a* (E-H), and *hand2* (I-L) in dorsal view. The AP length of *scl-1* expression in HS controls (black bracket, A) is truncated in length in Hsp70.cdx4 (B). Compared to the expression length of *scl-1* in DMSO controls (C) *scl-1* expression is also truncated in Talarozole-treated embryos (red arrowhead, D). The anterior boundary of *tbx5a* expression in the aLPM relative to expression in the eye (black bracket, E) is shifted rostrally in Hsp70.cdx4 (red arrowhead, E), compared to HS controls (E). Expression of *tbx5a* in the aLPM of Talarozole-treated embryos (red arrowhead, H) is also shifted rostrally, compared to DMSO-treated controls (G). The anterior boundary of *hand2* in the aLPM is unaffected between HS controls and Hsp.70.cdx4 (I, J). Expression of *hand2* shifts rostrally in Talarozole-treated fish (red arrowhead, L) compared to DMSO-treated controls (K). Expression of *tbx5a* in the pLPM at 18hpf is shifted rostrally in Hsp70.cdx4 embryos (red arrowhead, N) compared to HS controls (white arrowheads, M). Expression of *tbx5a* is also shifted rostrally in Talarozole-treated fish (red arrowhead, P) compared to DMSO-treated controls (white arrowheads, O). (Q) Quantification of the AP length of *scl-1* in the aLPM normalized to the trunk width (brackets in A). (R) Quantification of the length between *tbx5a* expression in the aLPM and eye (bracket, E),

normalized to the width of the trunk. Statistical significance was determined using the student t-test (*, p<.05, ***, p<.001, ****P<.0001. Scale bars represent 100um.

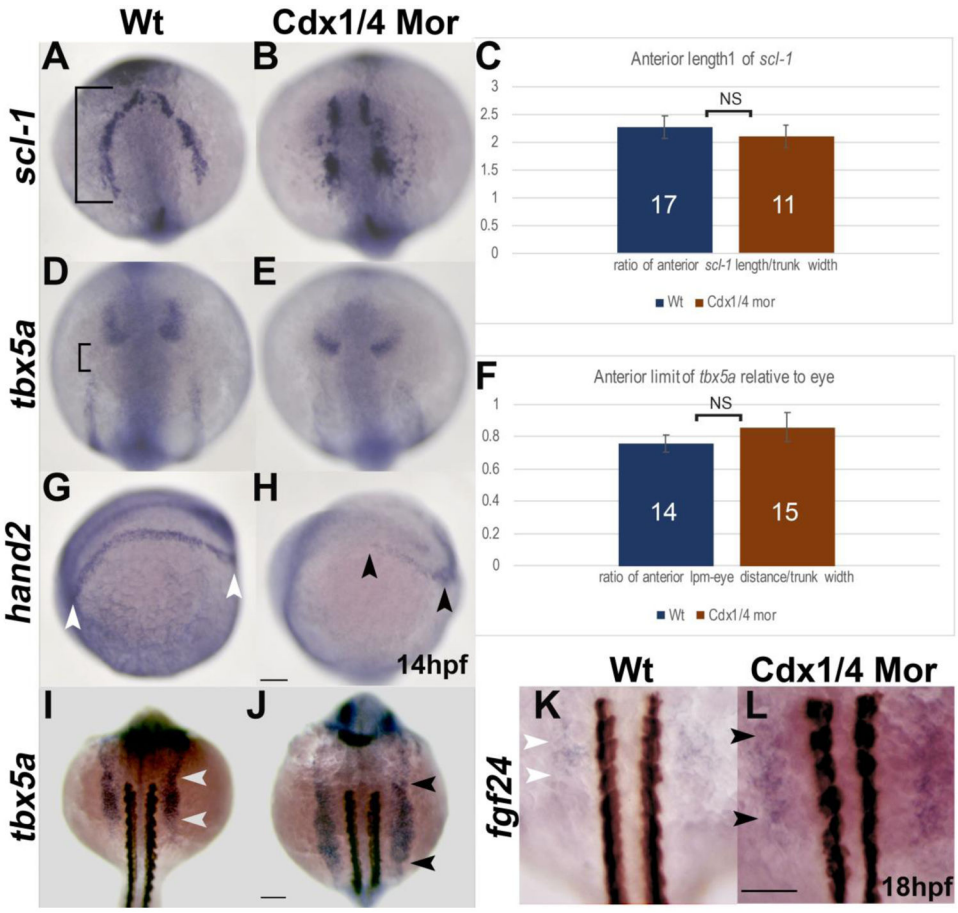

Fig. 4.

Cdx-deficient embryos have patterning defects in the pLPM. In situ hybridizations for *scl-1*(A, B) *tbx5a* (D-E) and *hand2* (G, H) at 14hpf as well as *tbx5a* (I-J) and *fgf24* (K, L) at 18hpf. (A,B) Wt and Cdx-deficient embryos are comparable in the AP length of *scl-1*. (C) Quantification of the AP length of *scl-1* (black bracket, A) normalized to the trunk width for wt and Cdx-deficient embryos. Expression of *tbx5a* relative to the eye is unaffected between wt and Cdx-deficient embryos (D, E). (F) Quantification of the AP length between *tbx5a* in the aLPM and the eye (bracket, D) shown as a ratio of the distance between the aLPM and the anterior eye, normalized to the width of the trunk, is comparable between wt and Cdx-deficient embryos. (G, H) The expression length of *hand2* in the pLPM is reduced in Cdx-deficient embryos (black arrowheads, H) compared to expression in wt (white arrowheads, G). (I, J) Expression of *tbx5a* at 18hpf is expanded posteriorly in the pLPM of Cdx-deficient embryos (black arrowheads, J), compared to wt (white arrowheads, I). (K,L) Expression of *fgf24* at 18hpf is expanded along the AP axis in Cdx-deficient embryos to somite levels 2-4 (black arrowheads, L) compared to wt where *fgf24* is expressed at the level of somites 2-3 (white arrowheads, K). Embryos are oriented in a dorsal view (A-B, D-E, I-L) or laterally with the anterior end towards the left (G-H). Non-significant differences in the quantitative analysis are indicated as NS. Scale bars represent 100um.

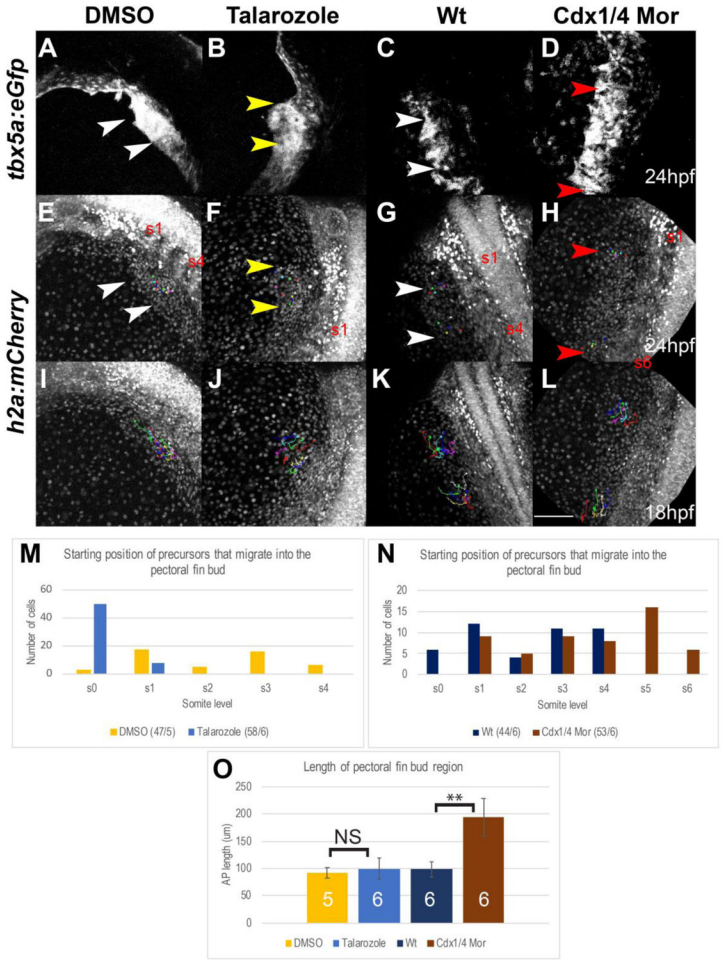

Fig. 5.

A subpopulation of Tbx5a-positive cells fails to migrate from the pLPM to the pectoral fin bud in Cdx-deficient embryos. (A-L) Maximum Intensity Projections (MIPs) of live-imaged *Tg(tbx5a:eGFP), Tg(h2afx:h2afv-mCherry)mw3* double transgenic embryos, oriented dorsally. The fin field cells that completed migration into the fin bud region are indicated by the arrowheads in *Tg(tbx5a:eGFP)* (A-D) and *Tg(h2afx:h2afv-mCherry)*mw3 (E-H) embryos at 24hpf. Cells that were backtracked beginning at 24hpf are indicated by the colored dots (E-H). The tracks for the selected cells are indicated by colored lines in *Tg(h2afx:h2afv-mCherry)mw3* embryos at 18hpf (I-L). The fin bud region at 24hpf is shown for wt (white arrowheads, A, E), Cdx-deficient (red arrowheads, B,F), DMSO-treated (white arrowheads, C, G), and Talarozole-treated (yellow arrowhead, D, H). The somite level of the anterior and posterior fin bud region is indicated (either s1 and s4 or s1 and s6). The somite level that Tbx5a-positive cells of the fin bud originated from at 18hpf are quantified for DMSO and Talarozole-treated embryos (M) or for wt and Cdx-deficient embryos (N). The number of cells tracked/the number of embryos used is indicated per condition as a fraction at the bottom of tables M-N. (O) Quantification of the length of the fin bud region at 28hpf for DMSO (yellow), Talarozole (blue), Wt (navy blue) and Cdx-deficient (brown). Statistical significance was determined using the student t-test (**, p<.01) Non-significant differences are indicated as NS. Scale bar represents 100um.

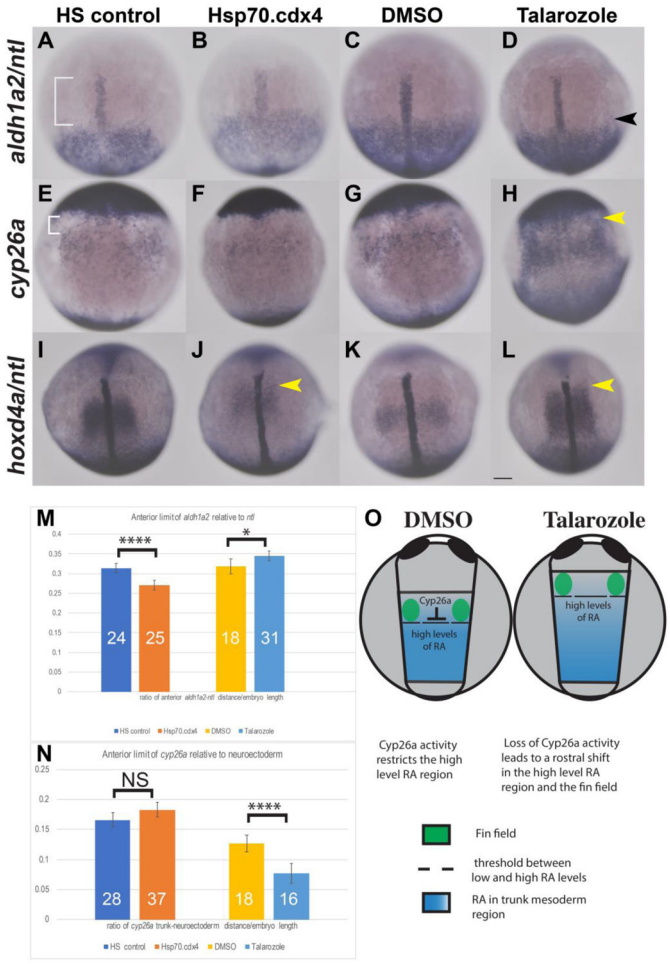

Fig. 6.

Overexpression of Cdx4 results in different effects on gene expression compared to increased RA . In situ hybridization for *aldh1a2* (A-D) shows the anterior boundary of expression relative to expression of *ntl* in the notochord (white bracket, A) shifts rostrally in Hsp70.cdx4 (B) compared to HS controls (A). *Aldh1a2* expression shifts caudally in Talarozole-treated embryos (black arrowhead, D) compared to DMSO-treated controls (C). The distance between the rostral boundary of *aldh1a2* and *ntl* expression was quantified and normalized relative to the yolk diameter in M. (E-H) Expression of *cyp26a* in trunk mesoderm relative to the anterior neuroectoderm is unaffected in Hsp70.cdx4 (F) compared to HS controls (white bracket, E). *Cyp26a* expression the trunk mesoderm of Talarozole-treated fish (H) is upregulated and shifted rostrally compared to DMSO-treated controls (G). The distance between expression in the trunk mesoderm and neuroectoderm was quantified in N (white bracket in E). (I-L) Expression of *hoxd4a* is shown relative to *ntl* expression and rostral shifts are indicated by yellow arrowheads (J, L). (O) Diagram of the presumed RA distribution (blue) relative to Cyp26a and the fin field (green) in DMSO and Talarozole-treated embryos at the tailbud stage. The threshold between high and low levels of RA is indicated by dashed lines. Embryos are shown in dorsal view with anterior torwards the top. Statistical significance was calculated using student t-test (*, p <.05, ****, p<.00001). Non-significant differences are indicated NS. Scale bar represents 100um.

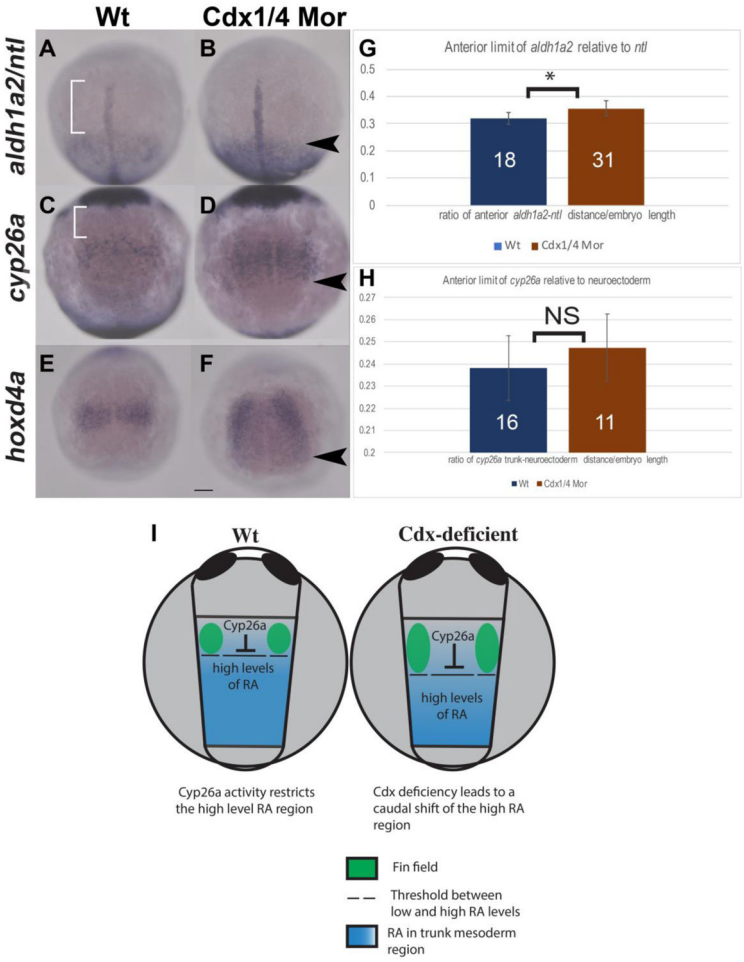

Fig. 7.

Cdx-deficiency results in a caudal shift in *aldh1a2* expression as well as a caudal expansion of *cyp26a* and *hoxd4a* at the tailbud stage (A-F). In situ hybridization for *aldh1a2* (A-B), *cyp26a* (C-D), at the tailbud stage and *hoxd4a* at 1-2ss (E-F). Expression of *aldh1a2* relative to the notochord shifts caudally in Cdx-deficient embryos (black arrowhead, B), compared to wt (white brackets, A). The length between the anterior boundary of *aldh1a2* and the notochord (white brackets) was quantified and normalized to the yolk diameter (G). Expression of *cyp26a* in the trunk mesoderm was compared relative to expression in the anterior neuroectoderm (C, D). The rostral boundary of *cyp26a* in the trunk was unaffected in Cdx-deficient embryos (D) compared to wt (C), although the posterior boundary of *cyp26a* expanded caudally. The length between *cyp26a* in the trunk mesoderm and neuroectoderm (white bracket in C) was quantified and normalized to the yolk diameter (H) and no significant differences were observed. Expression of *hoxd4a* expanded caudally in Cdx-deficient embryos (black arrowhead, F), compared to wt (E). (I) Diagram of the presumed RA distribution (blue) relative to Cyp26a and the fin field (green) in wt and Cdx-deficient embryos at the tailbud stage. Embryos are shown in dorsal view, anterior to the top and dashed lines indicate the threshold between low and high levels of RA. Statistical significance was calculated by using the student t-test, (*, $p < .05$). Non-significant differences are indicated as NS. Scale bar represents 100um.

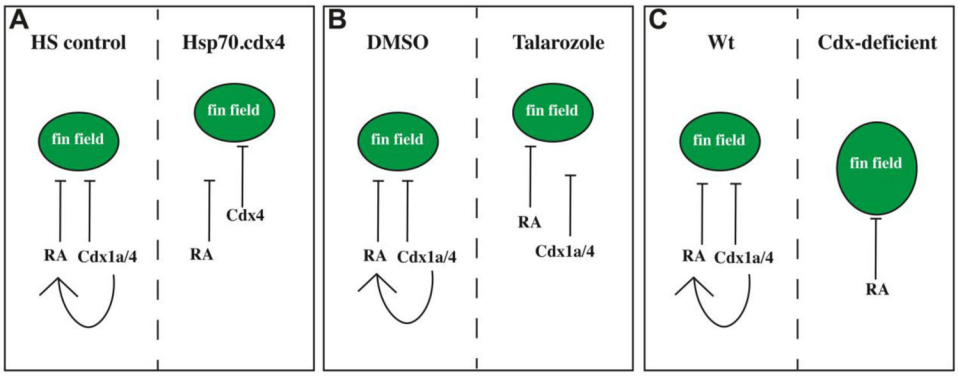

Fig. 8.

Cdx and RA act in parallel to position the pectoral fin field. (A-C) Summary diagram illustrating the presumed high level RA region and the region of Cdx1a/4 relative to the location of the fin field (green) at the tailbud stage. The control conditions are indicated on the left half (A-C), the rostrally shifted fin field (A-B) or the caudally expanded fin field conditions (C) are indicated on the right half. The inhibitory arrows indicate a role in restricting the location of the fin field and the arrow from Cdx1a/4 to RA indicates a role in maintaining the normal expression boundary of *aldh1a2* in that region of the embryo. Anterior is towards the top.